Developing a reactivatable model for HIV-1 Env expression mimicking latent infection

2022-05-13

Author	D.T. Roovers Bsc.
Daily supervisor	D. Postmus Bsc. Hons.
Examiner	prof. dr. C. Goffinet
Second examiner	dr. J. Symons

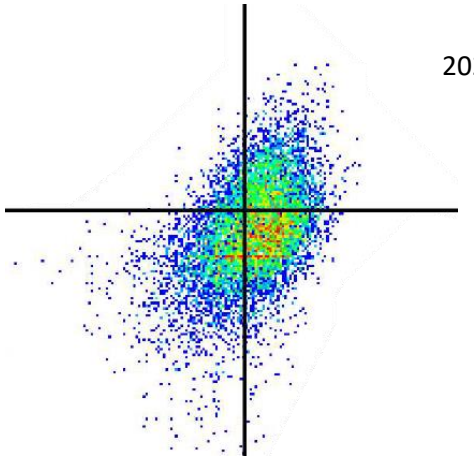

Abstract

The development of latent infection allows HIV-1 to evade the immune system, providing a major obstacle in the search for curative treatment. The so-called 'shock and kill' strategy tackles this problem by reactivating HIV-1 gene expression in latently infected cells, relying on cytopathic effects and the immune system to clear infected cells. Surface presentation of the HIV-1 envelope glycoprotein may be essential to this strategy, as Env is the only viral protein expressed on the cell surface during infection. In this study, Jurkat T-cells were modified to express HIV-1 Env containing an optimised GFP reporter in the fifth variable loop of gp120, driven by the authentic HIV-1 Tat-dependent LTR promoter. Env expression was induced by Panobinostat treatment, indicating that the cell line may serve as a model for Env expression in latently infected and reactivated cells. Treatment with interferon-α-2a was shown to affect the expression of Env during reactivation. The creation of this model cell line presents a powerful tool for research into HIV-1 Env. In furtherance of the 'shock and kill' strategy, a genome wide screen could be performed to identify host factors that affect Env surface levels during latency reversal. The generated cell line was transduced with lentiviral vectors introducing a CRISPR-based knockout of *GBP5*, resulting in a considerable reduction in basal and IFN-induced expression. In later research, these KO cells can be used to demonstrate the interplay of Env expression with known restriction factors of Env in the context of HIV-1 reactivation.

Introduction

To this day, no curative treatment exists for HIV (Deeks et al., 2021). While lifelong treatment with antiretroviral therapy (ART) successfully suppresses replication of the virus within patients and can prevent infection of others, many patients do not have access to the permanent medical attention ART treatment requires (Albert et al., 2014; Davey et al., 1999; unaids.org, 2022). Besides, chronic inflammation caused by HIV infection has been related to increased probabilities to develop cardiovascular and neurodegenerative disease in spite of viral suppression by ART, further underpinning the need for a cure for HIV (Babu et al., 2019; Barabona et al., 2021; Desplats et al., 2013).

A major obstacle in the search of a cure for HIV is the development of latency in a proportion of infected cells, a reversible state of infection characterised by low or absent expression of viral genes (Cohn et al., 2020; R. F. Siliciano & Greene, 2011). Cells in this transcriptionally silent state avoid detection by the immune system and thus persist in the patient, even under ART treatment (Reeves et al., 2018; J. D. Siliciano et al., 2003). Latency develops when activated $CD4^+$ T-cells – the primary target for HIV-1 infection – survive infection long enough to revert back to a resting memory state. Most $CD4^+$ T-cells die rapidly after infection, due to cytopathic effects caused by the virus or the host immune response (Ho et al., 1995; Wei et al., 1995). The cells that survive become part of a viral reservoir that is maintained by the longevity of infected T-cells in combination with proliferative renewal (Brodin et al., 2016; Chomont et al., 2009; Liu et al., 2020). The stability of the HIV-1 reservoir over time allows viral replication to rebound within weeks after ART is interrupted or abrogated, causing renewed viraemia in the patient (Davey et al., 1999; Pinkevych et al., 2015). On a molecular level, latency is thought to be maintained by a variety of processes, including inefficient export of multiply spliced RNA in resting $CD4^+$ T-cells (Lassen et al., 2006), compaction of chromatin surrounding the viral integration site (Lint et al., 1996), recruitment of histone deacetylases to the provirus (Coull et al., 2000; Tyagi & Karn, 2007; Williams et al., 2006), DNA methylation (Kauder et al., 2009) and transcriptional interference (Lenasi et al., 2008).

One strategy to provide curative treatment to HIV-1 infected patients involves the elimination of latently infected cells through the so-called 'shock and kill'-strategy (Hamer, 2005; Y. Kim et al., 2018). This strategy entails the reactivation of viral gene expression and virion production using latency reversal agents (LRA), subsequently relying on viral cytopathic effects and the immune system, including cytotoxic mechanisms imposed by humoral and cellular immunity, to clear reactivated cells. LRAs reactivate cells through a variety of mechanisms, including the inhibition of histone deacetylases (Archin et al., 2017; Rasmussen et al., 2014; Søgaard et al., 2015), protein kinase C modulation (Gutiérrez et al., 2016), toll-like receptor (TLR) agonism (Meås et al., 2020). Bromodomain and extra-terminal domain (BET) inhibitors have also been shown to reverse latency (Huang et al., 2017).

Although a multitude of clinical studies have shown that reactivation of viral transcription in infected cells is possible *in vivo*, none of them achieved a considerable reduction in the size of the viral reservoir (Archin et al., 2017; Elliott et al., 2015; Gutiérrez et al., 2016; Rasmussen et al., 2014; Søgaard et al., 2015). It seems that activation of viral gene expression alone is insufficient to induce cell death. Several strategies are being explored to promote the elimination of reactivated cells by enhancing the immune response, including the administration of natural killer (NK) cells (J. T. Kim et al., 2022), T-cell vaccination (Leth et al., 2016) and immunotherapy (van der Sluis et al., 2017; Wightman et al., 2015). The administration of broadly neutralising antibodies (bnAbs) was proposed to decrease the size of the viral reservoir, as indicated by delayed viral rebound after treatment interruption (Halper-Stromberg et al., 2014).

Alternatively, reactivating cells could be made more susceptible to clearance by the immune system by making the cells more immunologically 'visible' upon reactivation. The envelope glycoprotein (Env) is the only viral protein expressed on the cell surface during productive infection, making it a primary target for antibody-dependent cellular cytotoxicity (ADCC) and other parts of the immune response (Beitari et al., 2019). HIV-1 has developed several viral evasion mechanisms that conceal infected cells by reducing surface presentation of Env, including rapid recycling of surface Env by endocytosis (Egan et al., 1996; Rowell et al., 1995) and dissociation of Env from the cell surface ('shedding') (Mckeating et al., 1991; Schneider et al., 1986). Besides, a plethora of anti-HIV-1 host restriction factors have been identified that affect the surface presentation of Env by targeting the maturation and trafficking of Env (Beitari et al., 2019). For instance, interferon induced transmembrane (IFITM) proteins interact with Env, inhibiting Env processing and incorporation of Env into virions (Yu et al., 2015). Guanylate binding protein (GBP) 5 alters the glycosylation of Env and inhibits cleavage similarly to the IFITM proteins, reducing surface levels of Env in infected cells (Krapp et al., 2016). Other restriction factors restrict Env expression by promoting endoplasmic reticulum-associated degradation (ERAD) of Env (Zhou et al., 2014, 2015) or downregulate Env from the cell surface (Tada et al., 2015).

Since the killing of HIV-1-infected cells relies in part on the accessibility of cell surface-presented Env, it follows that the direction of Env to the cell surface during latency reversal may be essential to putting the 'kill' in the 'shock and kill' strategy. Anti-HIV-1 restriction factors that counter viral evasion mechanisms or otherwise affect surface levels of Env during latency reversal may therefore affect the effectivity of said strategy. The identification of such host factors can be achieved by the execution of a genome-wide knockout (KO) screen, tracking the subcellular localisation of Env upon KO of every gene. An important prerequisite of such a study is the availability of a cell line that serves as a model for latent infection and is amenable to high throughput screening. Such a cell line should allow expression and surface presentation of the Env glycoprotein that is inducible by LRAs.

The objective of this research is to establish a BSL2-level model for latent HIV-1 infection, which allows for the identification of host factors that affect HIV-1 Env surface presentation during latency reversal. In order to achieve this, a transfer plasmid was created to express Env driven by the long terminal repeat promoter with the transcriptional enhancer Tat (LTR-TAT). Alongside this HIV-1-native expression system, an expression vector with the non-native human cytomegalovirus (CMV) immediate-early promoter was created. The use of both expression systems in parallel would allow for discrimination between host factors that affect the Tat-dependent LTR promoter in general or the maturation and trafficking of Env specifically. These expression vectors can be introduced into Jurkat T-cells, a cell line derived from leukemic $CD4^+$ T-cells (Abraham & Weiss, 2004). By equipping the expression vector with an HIV-1 Env-GFP fusion protein (EnvGFP), the expression and subcellular localisation of Env could be tracked by direct evaluation of the reporter by fluorescence microscopy and and antibody-dependent detection using intact cells, respectively. Insertion of GFP in the V5 loop of Env was demonstrated not to affect the expression or functionality of Env (Nakane et al., 2015). The J-lat cell line, a Jurkat subclone expressing GFP by the LTR-TAT expression system, is not suitable for this study, because while reactivation may be trackable using this cell line via the GFP surrogate, the production and localisation of Env are not (Jordan et al., 2003).

The planned genome-wide KO screen would be performed by transduction of a pooled library of single guide RNA (sgRNA) sequences alongside the Cas9 nuclease into the EnvGFP-expressing Jurkat T-cells. Similar CRISPR based screens have been used in previous research to identify HIV host dependency factors

and host factors mediating interferon (IFN) inhibition (OhAinle et al., 2018; Park et al., 2016). Fluorescence-activated cell sorting (FACS) can be used to enrich for cells within the population, in which the expression or surface levels of Env are affected negatively and positively, after which over- or underrepresentation of genes with deletions can be identified by sequencing of the sgRNAs in the sorted populations. In further preparation for the KO screen, *IFITM1* and *GBP5* were partially knocked out in the EnvGFP-producing cells in an effort to generate KO cell lines. As these host factors are known to affect the surface presentation of Env (Krapp et al., 2016; Yu et al., 2015), they may be used to assess whether the model cell line is suitable to demonstrate the Env-modulating effect of known restriction factors.

Results

Molecular cloning of lentiviral EnvGFP expression vectors

Using digestion cloning, the NL4.3 Env V5.3 GFP OPT was inserted into a lentiviral expression vector with either a native LTR-TAT expression system or the CMV promoter (*fig. 1*). A PCR screen was performed to determine the optimal conditions for amplification of the EnvGFP insert for the CMV-driven construct (*supplementary fig. 1A*). Optimal yield and product specificity was achieved with an annealing temperature of 67°C. Ligation of the pHR' CMV backbone and the insert was validated by digestion (*fig. 1A*) and by sequencing. However, lipofection of the plasmid into HEK293T cells showed only 5% of GFP-positive cells with an MFI only marginally higher than the untransfected control, as determined by flow cytometry (*fig. 1B*). As a control, the parent plasmid (pHR' CMV-GFP) and a CMV-driven HXB2 Env V5.3 GFP OPT expression plasmid with a different backbone were transfected into HEK293T cells in parallel (*supplementary fig. 1B*). All positive controls performed as expected, with the CMV parent plasmid giving 47% GFP-positive cells, the LTR-TAT parent plasmid 16% and the CMV-HXB2 Env plasmid 79%. In an effort to improve the expression of the CMV-EnvGFP plasmid, a kozak sequence was inserted before the start codon of the Env gene by site directed mutagenesis. Transfection into HEK293T cells showed this provided no improvement in Env expression (data not shown).

To obtain a lentiviral expression vector with LTR-TAT-driven EnvGFP, a conventional cloning strategy similar to for CMV-EnvGFP was employed. The NL4.3 Env V5.3 GFP OPT insert was amplified with varying amounts of template (*supplementary fig. 1C*). An optimal yield and product specificity was achieved with 50 ng of template. The lentiviral LTR-TAT backbone was digested with *Xho*I and *Msc*I. Subsequent ligation reactions with the aforementioned insert and backbone yielded no colonies after transformation. Several parameters were varied to no avail, like the insert:vector molar ratio and the volume of ligation mix to be transformed into competent bacteria.

To exclude the need for ligation, an InFusion cloning strategy was pursued instead. The NL4.3 Env V5.3 GFP OPT insert and backbone were amplified by PCR and inverse PCR, respectively. Primers were used to provide the insert with ends complementary to the backbone, allowing the fragments to anneal during an InFusion reaction. Several PCR screens were performed to optimise the yield of the backbone amplification (*supplementary fig 1D*). The InFusion reaction mix was transformed into Stbl. II cells. A digestion test with *Xho*I and *Msc*I and Sanger sequencing of the product both indicated that the produced plasmid now contained both the inserted EnvGFP and eGFP (*fig. 1C*, upper DNA sequence and digestion test), which was supposed to be eliminated from the backbone by inverse PCR. eGFP was removed from the produced plasmid by digestion with *Msc*I, gel purification and subsequent religation. The correctness

of the plasmid was validated by another digestion test with *Msc*I and *Xho*I and Sanger sequencing (data not shown).

23% of HEK293T cells transfected with the LTR-TAT-driven EnvGFP plasmid were GFP-positive, with an increase in MFI of 70% with respect to the mock treated cells (*fig. 1B*). 14% of transfected cells presented EnvGFP on the cell surface, as determined by an α-GFP APC surface staining (*fig. 1C*, trial transfection). The MFI of the surface staining increased by 83% with respect to the mock (data not shown).

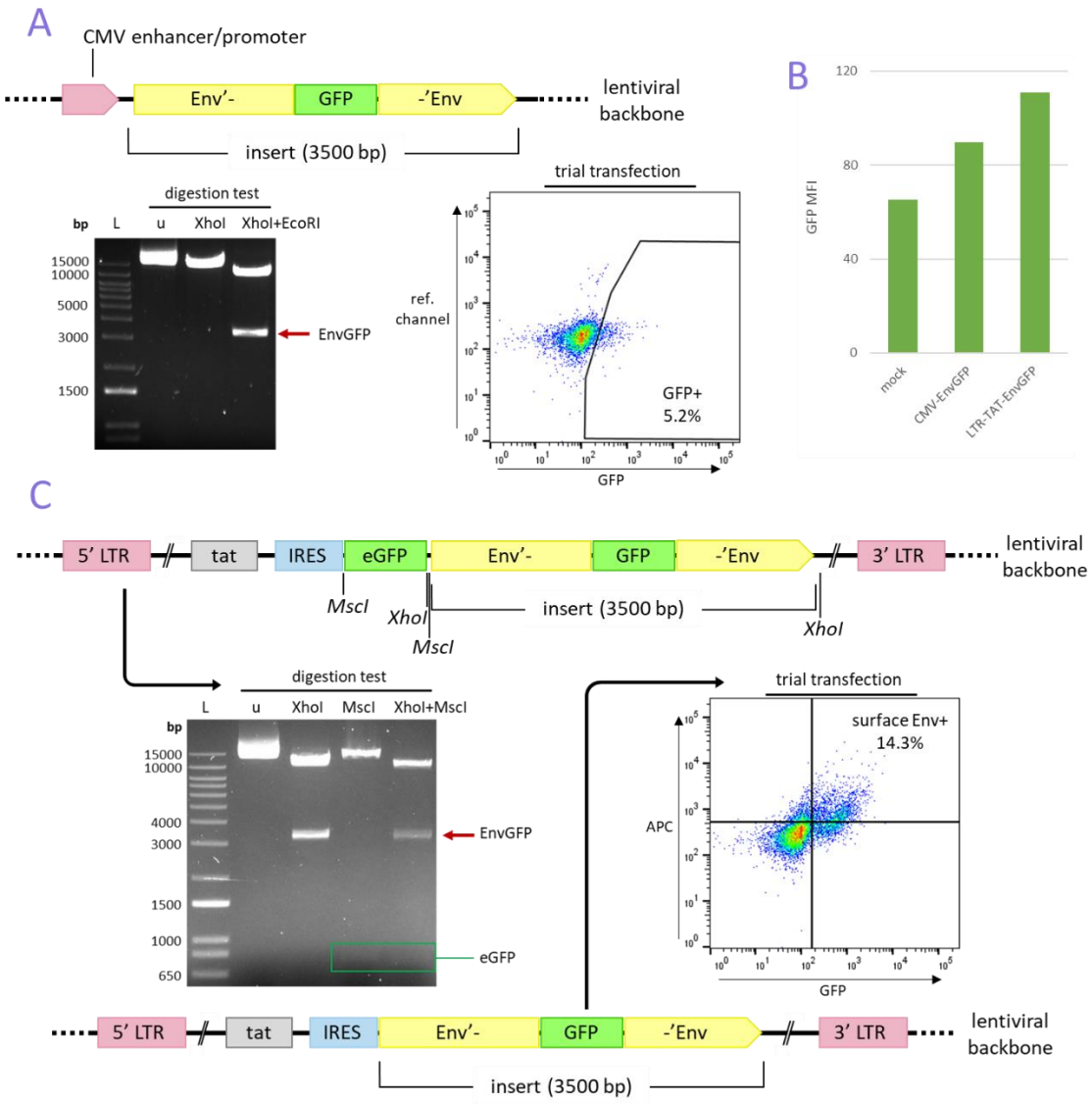

Figure 1: Cloning of lentiviral EnvGFP expression vectors. A: A CMV-driven EnvGFP construct was created by restriction enzyme cloning and validated by digestion with XhoI and EcoRI. The expression of plasmid was assessed by transfection into HEK293T cells. B: GFP MFI of the CMV- and LTR-TAT-driven expression vectors upon transfection into HEK293T cells compared to mock treated cells, as determined by flow cytometry. C: InFusion cloning inserted the EnvGFP insert into the LTR-TAT-driven backbone without removing the eGFP gene (upper sequence). The structure of this plasmid was determined by a digestion test using XhoI and MscI. eGFP was removed from the structure by digestion (lower sequence), after which the expression of the plasmid was assessed by transfection into HEK293T cells. Env surface levels were determined by an α-GFP APC surface staining.

Generation and characterization of a latently EnvGFP-expressing Jurkat T-cell line

VSV-G-pseudotyped lentiviral particles were generated, carrying either the LTR-TAT or pHR' CMV driven EnvGFP expression vectors as transfer plasmids. Parental Jurkat T-cells were transduced with increasing amounts of pseudoviral particles in the presence or absence of polybrene, a cationic enhancer of viral transduction efficiency (Davis et al., 2002). A considerable amount of cells was found to express EnvGFP one day after transduction, as judged by fluorescence microscopy (*fig. 2A*). Five days after transduction, a maximum of 12.8% and 2.8% of cells transduced with the LTR-TAT and CMV driven EnvGFP plasmids, respectively was GFP-positive (*fig. 2B*). In total, the cells were cultured and expanded over eight days without antibiotic selection and subsequently sorted for GFP-positive cells using fluorescence assisted cell sorting (FACS). *Fig. 2C* shows the cells that were processed by the FACS device, including the gate that was used to select GFP-positive cells. GFP-positive cells with high fluorescence in the reference channel (R670) were excluded from this gate to prevent selection of autofluorescing cells by FACS. Interestingly, the GFP-positive fraction of the transduced cells was higher when analysed at the cell sorting facility than as determined before. While the gating between the two experiments (*fig. 2B* and *C*) is not the same, the difference may also be explained by the death of highly autofluorescing cells in the days between the flow cytometric analysis (*fig. 2B*) and FACS (*fig. 2C*).

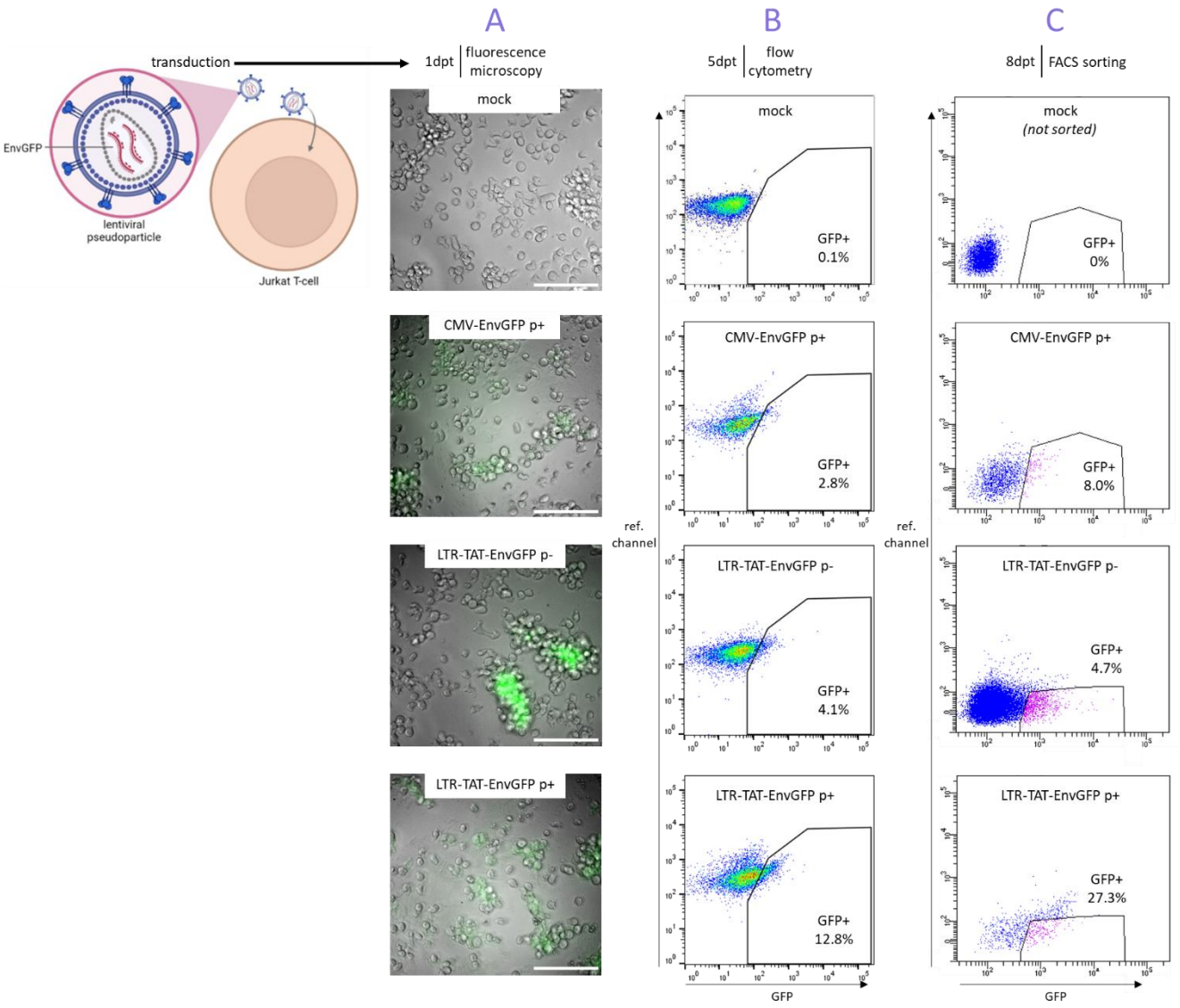

Figure 2: Towards generation of latently Env-GFP-expressing Jurkat cell lines. Transduced and mock-treated cells were analysed by fluorescence microscopy two days after transduction (A) and by flow cytometry five days after transduction (B). Eight days after transduction, GFP-positive cells were enriched for by FACS (C).

A FACS-sorted 'bulk' population of 4800 LTR-TAT EnvGFP Jurkat T-cells was subjected to 4, 24 and 48 h of treatment with 50 nM Panobinostat, harvested after 48 h and analysed using flow cytometry (*fig. 3*). Both the fraction of GFP-positive cells and the GFP MFI increased dramatically upon reactivation in a treatment duration-dependent manner.

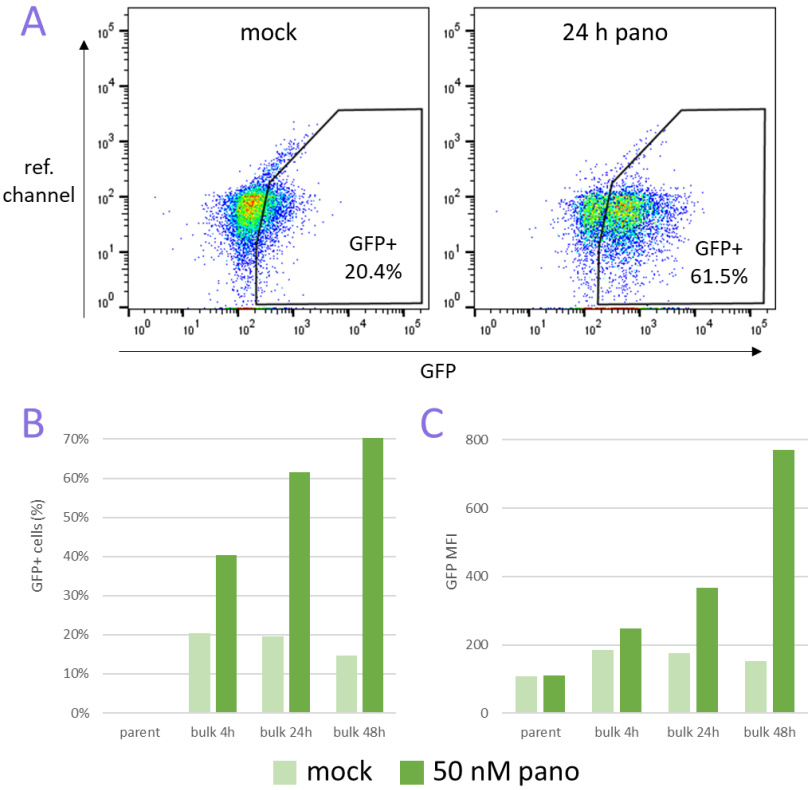

Figure 3: EnvGFP expression in FACS-sorted population of LTR-TAT EnvGFP Jurkat T-cells is activatable by Panobinostat treatment. Cells were reactivated by treatment with Panobinostat for 4 to 48 h and analysed using flow cytometry (A). The fraction of GFP-positive cells (B) and the GFP MFI (C) increased with longer Panobinostat treatment.

Of the 192 LTR-TAT-driven single-cell clones generated by sorting, seven were expanded for further characterisation. The clones were treated with 50 nM Panobinostat for 24 hours and analysed by flow cytometry, western blot and reverse transcription quantitative PCR (RT-qPCR) to assess their capacity for reactivation (*fig. 4*). As an arbitrary cut-off to aid the flow cytometric analysis, a population of cells was considered to reactivate when it displayed >20% GFP-positive cells upon reactivation and a two-fold increase in GFP positivity and GFP MFI during reactivation. The fraction of GFP-positive cells was below 4% in all mock-treated clones, except clone VI (*fig. 4A*). Five out of seven clones (II, III, IV, VI and VII) reactivated after treatment with Panobinostat, with GFP positivity after reactivation ranging between 48% and 98% and a GFP MFI increase between 2.3- and 9.1-fold (*fig. 4A*, *B*).

To assess the effect of reactivation on surface presentation of EnvGFP, all clones were surface-stained with an α-GFP antibody conjugated to APC. In clone III, Panobinostat treatment caused the fraction of surface Env-positive cells to increase from 0.5% to 23% (*fig. 4A*) with a 3.7-fold increase in APC MFI (data not shown), suggesting that Panobinostat treatment strongly induced surface expression of EnvGFP. While clones II, IV, VI and VII also show a GFP- and APC-positive population upon reactivation, a considerable fraction of GFP-negative cells in these clones unexpectedly displayed strong signal in the APC-channel, both with and without Panobinostat treatment (*fig. 4A* and *supplementary fig. 2A*). In spite of this, the increase in surface-Env positive cells upon reactivation outweighed the size of the GFP-negative APC-positive population in clones II, VI and VII, indicating that Panobinostat treatment induced

surface expression of EnvGFP in these clones. Notably, each sample was accompanied by an unstained control to assist the gating and multiple washing steps were performed to reduce background signal. In another experiment, surface staining was performed using an α-Env antibody (2G12) for comparison. Reactivation increased the fraction of surface Env-positive cells in clones II, III, IV, VI and VII (*supplementary fig. 2B*). In clones II, IV, VI and VII, a fraction of GFP-negative cells was positive for the α-Env surface staining, similar to what was observed with the α-GFP surface staining.

The reactivation experiment was repeated with a readout by western blot (*fig. 4C*). Env expression was determined by α-gp120 immunostaining, with the housekeeping protein GAPDH serving as a loading control. Western blot analysis corroborated the finding, that clones II, III, IV, VI and VII respond most strongly to reactivation by Panobinostat, with signal for the α-gp120 staining increasing between 6.5 and 14.4-fold. In another repetition of the reactivation experiment, the effect of Panobinostat treatment on Env transcript levels was determined using RT-qPCR (*fig. 4D*). Again, the strongest reactivation was observed for clones II, III, IV, VI and VII. The log2 expression change ranged between 5.1 and 39.6. Though this is a notably stronger increase than detected at the protein level by western blot or flow cytometry, this difference can be explained by the fact that protein levels do not directly correspond to the amount of mRNA in the cell.

None of the twelve CMV-EnvGFP single-cell clones obtained from the cell sorting facility survived and expanded. Of the 36 multi-cell clones obtained by FACS, two five-cell cultures and two ten-cell clones were expanded for further characterisation. The multi-cell clones were stimulated with 24 h of treatment with 50 nM Panobinostat. The fraction of GFP positive cells remained below 2% for all clones, with no significant increase in MFI with respect to the parental Jurkat T-cells (data not shown), suggesting that an insufficient amount of cells integrated the CMV-EnvGFP vector after transduction.

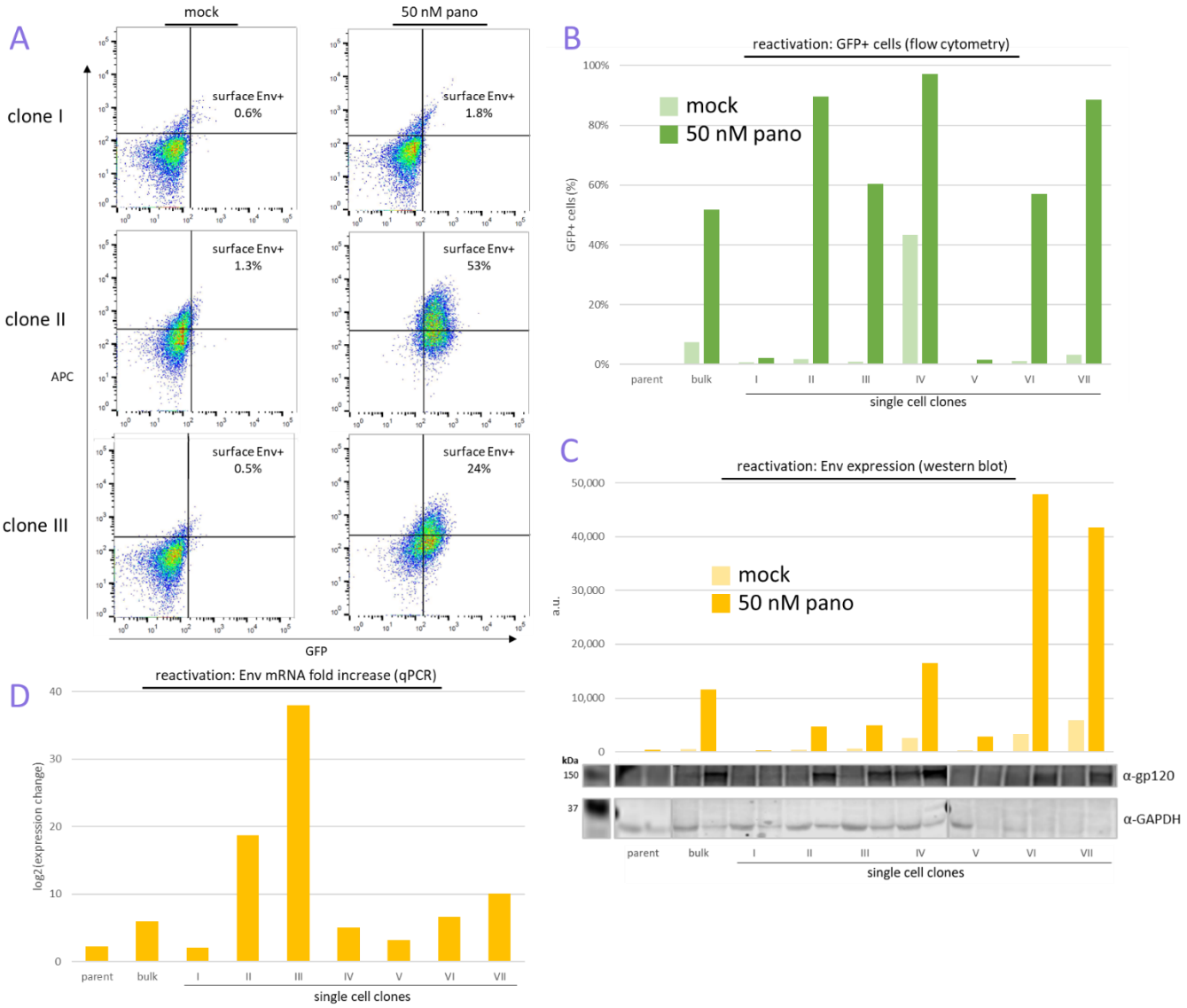

Figure 4: Panobinostat treatment strongly induces EnvGFP expression in five out of seven LTR-TAT EnvGFP Jurkat T-cell clones obtained by FACS. Cells were reactivated by treatment with Panobinostat and Env expression was analysed by flow cytometry (A, B), western blot (C) and RT-qPCR (D). All three analytical methods demonstrated that Panobinostat treatment induced expression of Env in clones II, III, IV, VI and VII, as well as in the bulk population obtained from cell sorting.

In order to assess the effect of the interferon response on LRA-induced EnvGFP expression in the LTR-TAT EnvGFP Jurkat T-cells, the cells were pre-treated for 24 h with 250 IU/mL interferon-α-2a before reactivation and analysed by flow cytometry (*fig. 5*). Since cellular stress caused by the interferon response is known to increase autofluorescence (Surre et al., 2018), the MFI of the IFN-treated, reactivated cells was corrected for the difference in fluorescence between the mock- and IFN-treated controls (see *Experimental Method – Reactivation of Jurkat T-cells*). Only the clones that reactivated strongly by Panobinostat treatment as determined before (II, III, IV, VI and VII) were considered. On average, all clones displayed a reduced MFI during reactivation when pre-treated with IFN-α-2a, suggesting that the interferon response may restrict reactivation of EnvGFP expression. The effect was negligible when taking the variance (arithmetic mean, SD) between the repeated experiments (n = 2) into account, however. More repetitions are required to obtain statistically relevant results.

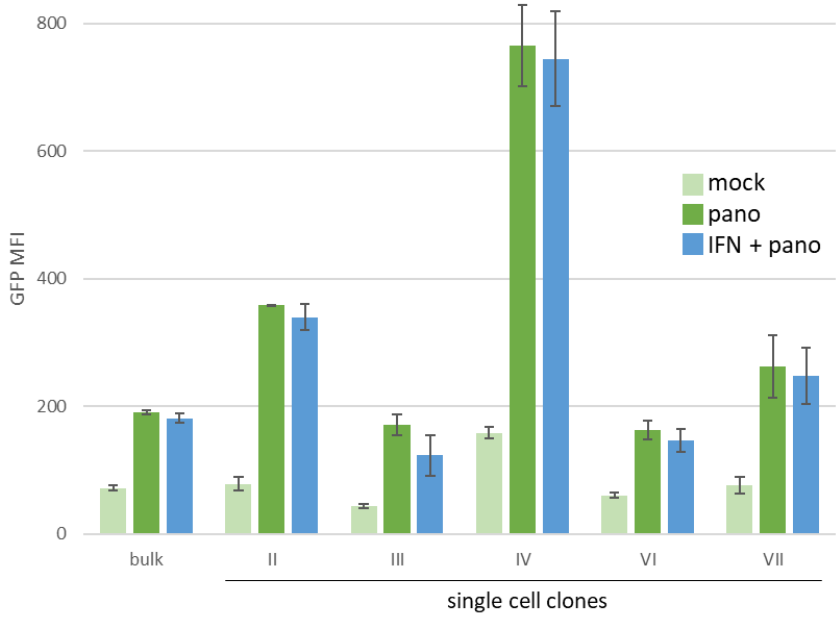

Figure 5: The interferon response may affect LRA-induced EnvGFP expression in LTR-TAT EnvGFP Jurkat T-cells. Cells were reactivated by 50 nM Panobinostat after pre-treatment with 250 IU/mL IFN-α-2a and analysed by flow cytometry (n = 2, arithmetic mean, SD). A minor decrease in average EnvGFP expression was observed in all clones, more repetitions are required to obtain statistically relevant results.

Partial knock-out of IFITM1 and GBP5 in LTR-TAT EnvGFP Jurkat T-cells

To demonstrate the interaction between EnvGFP expression in the LTR-TAT EnvGFP Jurkat T-cells and known restriction factors IFITM1 and GBP5, the bulk population of the LTR-TAT EnvGFP Jurkat T-cells was transduced with increasing amounts of lentiviral KO particles against IFITM1 and GBP5 in the presence or absence of polybrene. Transduced cells were expanded and subjected to puromycin selection (1 µg/mL). Twenty days after transduction, cells were harvested and analysed by western blotting (*fig. 6*). The bulk populations were pre-treated with IFN-α-2a to assess the inducibility of IFITM1 and GBP5 in the parental cells and assure absence of their expression in the KO cells. While the basal expression levels of IFITM1 were below the detection limit for both the parent and knock out populations, a detectable amount of IFITM1 was expressed in the parental cells after IFN stimulation (*fig. 6A*). The IFN induced expression of IFITM1 was only 16% and 26% lower in IFITM1 KO populations I and II than in the parental population (*fig. 6A*), suggesting failure of knock-out.

In the case of GBP5, expression was increased 2.8-fold due to IFN treatment. In the KO populations, the basal expression was reduced by 49% and 55% with respect to the parent population, while the IFN induced expression was 61% and 72% lower (*fig. 6B*). The basal expression of Env increased by 24% with respect to the parent population in the first GBP5 KO population and decreased by 7% in the second (*fig. 6C*). Band intensities were insufficient for analysis of gp160 processing. Treatment with IFN reduced the expression of Env by 55% in the parent population. While a comparable reduction was observed in the first GBP5 KO population, a reduction of only 20% was observed in the second GBP5 KO population, suggesting that the restriction of Env expression by the interferon response was weakened considerably by the knock-out.

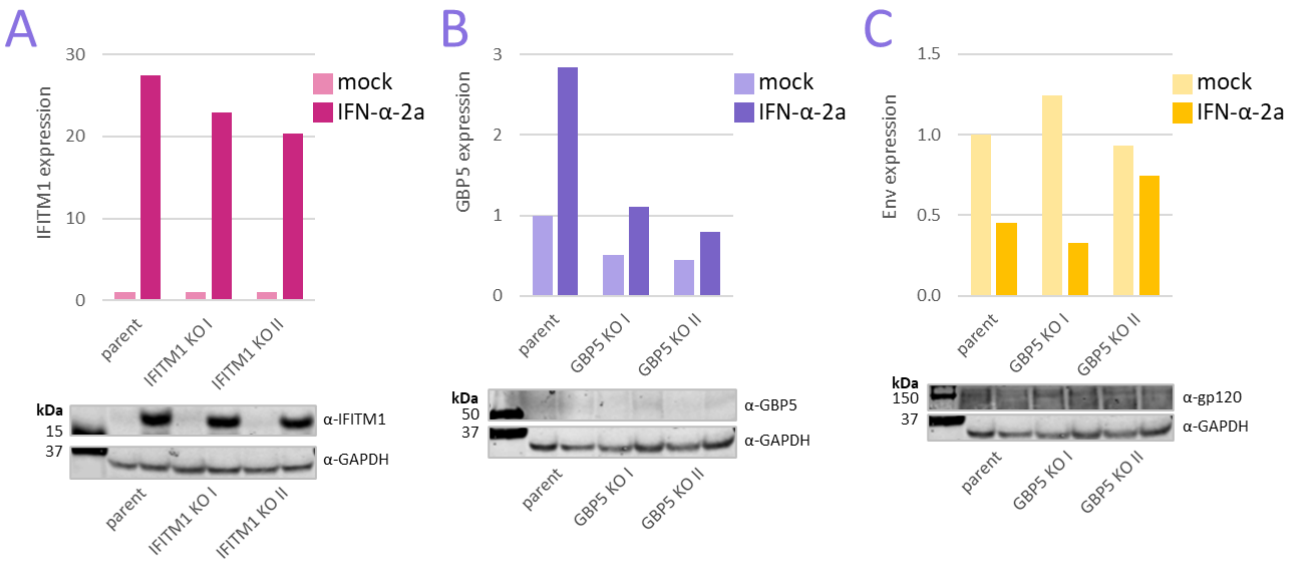

Figure 6: GBP5 partially knocked out of LTR-TAT EnvGFP Jurkat T-cells; unsuccessful KO of IFITM1. Restriction factor expression was determined after stimulation by IFN-α-2a using western blot analysis for both IFITM1 (A) and GBP5 (B). A moderate decrease in basal expression was observed for GBP5 and IFN induced expression was reduced for all IFITM1 and GBP5 KO populations. In the same experiment, the basal and IFN induced expression of Env was measured (C). Whereas the IFN response reduces Env expression by 55% in the parent population, only 20% reduction was observed in the second GBP5 KO population.

Discussion

In this research, the Jurkat T cell line was manipulated by transduction to express NL4.3 Env V5.3 GFP OPT by the authentic HIV-1 Tat-dependent LTR promoter. The cells displayed low basal and high LRA-induced expression of EnvGFP. Though more extensive characterisation of the created cell lines is required, the findings described here present an important step towards a better understanding of the expression of envelope glycoprotein of HIV-1 in latently infected cells. The LTR-TAT-driven EnvGFP Jurkat T-cells can be used to further prepare for the genome wide screen to identify host factors affecting the surface presentation of HIV-1 Env. A first step in this direction could be finding the ideal combination of LRAs to effectuate optimal latency reversal. While numerous publications have investigated the optimal conditions for latency reversal, these findings will have to be validated with the created cell line (Cary & Peterlin, 2018; Khanal et al., 2021; Kula et al., 2019).

The heterogeneity of the latent reservoir forms a major obstacle to achieving targeting of all infected cells by latency reversal agents (Ait-Ammar et al., 2020; Grau-Expósito et al., 2019). Besides T-cells, cell types like tissue macrophages, myeloid cells and hematopoietic stem cells are thought contribute to the persistence of HIV-1 (Hendricks et al., 2021; Kuo & Lichterfeld, 2018). Although execution of the genome-wide screen with the EnvGFP-expressing Jurkat T-cells will be an important step towards the identification of host factors that affect Env during latency reversal, the use of different cell types in parallel may allow for a more comprehensive readout. In addition to this, it is important to note that considerable heterogeneity also exists within infected $CD4^+$ T-cells. The integration of the provirus in different parts of the host genome plays a determining role in the reactivation dynamics of each individual cell (Chen et al., 2016). In this context, the use of a bulk population of transduced cells in lieu of a cell line presents a more elegant tool for research, as the bulk population will naturally harbour a wide array of integration sites. Alternatively, a combination of cell lines representing different integration sides could be used in the genome wide screen.

Besides their application in the genome wide screen, the EnvGFP-expressing Jurkat T-cells may also be put to use in other research. The cells could, for instance, be used to study therapeutics that improve the surface presentation of Env during latency reversal. This would make reactivating cells more susceptible to clearance by the immune system, thereby strengthening the 'shock and kill' strategy. Furthermore, the EnvGFP-expressing cells created in this research provide an important advantage over the J-lat cell line when investigating latency reversal. In patients, productively infected cells are eliminated due to targeting by the immune system, but also as a result of the cytopathic effects of the production of viral proteins, including Env (Costin et al., 2007; Holm et al., 2004; Oyaizu et al., 1994). The newly created cells produce the toxic Env protein when latency is reversed, whereas J-lat cells produce GFP upon reactivation. This makes the EnvGFP producing Jurkat T-cells a more relevant model for studying the effects of latency reversal on cellular stress and viability in the context of the 'shock and kill' strategy.

Creating an LTR-TAT-driven EnvGFP-expressing cell line

An expression vector for LTR-TAT-driven NL4.3 Env V5.3 GFP OPT was created by InFusion cloning (*fig. 1B* and *C*). Stable expression of EnvGFP was achieved by transduction of the vector into Jurkat T-cells, followed by FACS (*fig. 2*). The bulk population and five out of seven single-cell clones were characterised by low basal expression of EnvGFP and displayed a strong increase in expression as a result of Panobinostat treatment, as determined by flow cytometry, western blot analysis and RT-qPCR (*fig. 3* and *4*). Considerable variance between the different clones was observed, ranging from unresponsive cells to

clones showing a dramatic increase in EnvGFP expression after treatment with Panobinostat. Unresponsive clones could be derived from unsuccessfully transduced cells that were erroneously selected by the FACS instrument. Alternatively, the EnvGFP construct integrated in a non-reactivatable region of the host genome, as has been proven to occur in primary HIV-1 infected T-cells (Battivelli et al., 2018). Lastly, the site of integration could be such that the histone deacetylation inhibition provided by Panobinostat is not able to induce expression (Chen et al., 2016). Further reactivation experiments using LRAs with a different mode of action (or combinations thereof) could be performed to determine whether single-cell clones that are not reactivatable by Panobinostat could be activated by other means.

Panobinostat is a histone deacetylase inhibitor (HDACi) that has been used to reactivate latently infected T-cells (Rasmussen et al., 2014; Spivak et al., 2015). The effectivity of Panobinostat in inducing EnvGFP expression in the bulk population and the majority of single-cell clones serves as a strong indication that processes similar to those maintaining latency in HIV-1 infected cells silenced the integrated EnvGFP insert in the transduced Jurkat T-cells, suggesting that the clones created in this research are suitable as models for latent infection.

In order to assess the surface presentation of EnvGFP in the bulk population and the single-cell clones, the cells were surface-stained with either an α-GFP APC or α-Env 2G12 AF633 antibody for flow cytometric analysis. The bulk population and the five clones that were shown to increase EnvGFP expression as indicated by the GFP MFI (II, III, IV, VI and VII) all displayed an increase in the fraction of surface-staining positive cells upon reactivation. In clone III, Panobinostat treatment increased the fraction of GFP- and surface staining-positive cells increased from 0.5% to 23%, indicating that the surface expression of EnvGFP was strongly LRA-inducible. In the other clones, a fraction of cells unexpectedly responded to the surface staining, despite being GFP-negative. This may distort the readout of the experiment in these particular clones, as it cannot be determined afterwards whether a GFP- and surface staining-positive cell is truly presenting EnvGFP on its surface, or merely displaying intracellular EnvGFP expression in combination with aberrant interaction with the surface staining. Nevertheless, the increase in surface Env-positive cells upon reactivation was larger than the population of GFP-negative and surface staining-positive cells in the case of clones II, VI and VII, indicating that surface presentation of EnvGFP was induced by Panobinostat. In the future, an isotype control like the rat IgG2a kappa eFluor 660 could be used to exclude signal derived from interactions that are not specific to the α-GFP epitope (thermofisher.com, 2022b). As this issue with surface staining was not observed in clone III, this cell line is most suitable for use in the genome-wide screen and other future research.

Interferon stimulation may weaken Env expression during reactivation

The effect of the interferon response on the LRA-induced EnvGFP expression was assessed by flow cytometry. The LTR-TAT driven EnvGFP Jurkat T-cells were pre-treated with IFN-α-2a and subsequently reactivated with Panobinostat. All reactivating clones displayed a minimal reduction in MFI increase during reactivation when pre-treated with IFN-a-2a (*fig. 5*), indicating that the interferon response may restrict EnvGFP expression during reactivation. More repetitions of this (duplicate) experiment should be performed to obtain statistically relevant results.

Many restriction factors induced by the interferon response affect the processing and surface presentation of Env (Krapp et al., 2016; Tada et al., 2015; Yu et al., 2015; Zhou et al., 2014, 2015). To further underpin the biological relevance of the created cell line, it will be interesting to use flow

cytometry with surface staining to investigate the effect of IFN-treatment on the surface presentation of EnvGFP during latency reversal.

Creating a CMV-driven EnvGFP-expressing cell line

To complement the LTR-TAT-driven EnvGFP-expressing cell line, several attempts were made to clone EnvGFP into an expression vector driven by a constitutive promoter that is not native to HIV-1, like the CMV promoter. While a CMV-driven expression plasmid based on the pHR' lentiviral backbone was created successfully, it performed poorly upon transfection into HEK293T cells (*fig. 1A* and *B*). Only very low expression levels were achieved, while the parental plasmid (pHR' CMV-GFP) and a CMV-driven EnvGFP plasmid with a different backbone performed as expected (*supplementary fig. 1B*). Sanger sequencing of the created plasmid did not reveal the presence of any aberrant nucleotides in the promoter and EnvGFP sequence. The insertion of a kozak sequence did not improve the expression levels. It remains unclear why the created expression vector performs poorly. In spite of its poor performance in transfection experiments, the CMV-EnvGFP plasmid was transduced into Jurkat T-cells in an effort to create a stable cell line. Perhaps not surprisingly, the multiple cell clones obtained from the cell sorting facility displayed negligible levels of EnvGFP expression after treatment with Panobinostat, as determined by flow cytometry (data not shown).

The use of a cell line expressing EnvGFP driven by CMV in parallel with LTR-TAT, an expression system native to HIV-1, is instrumental the identification of host factors that affect the surface presentation of Env during latency reversal. A cell line expressing EnvGFP via the LTR promoter alone is insufficient, as it would not be possible to discern whether any observed effect on Env surface presentation is due to a host factor interfering with Env processing and trafficking, or by interaction with the LTR-TAT expression system as a whole. Although it was not possible to generate a CMV-driven EnvGFP-expressing cell line, the J-lat cell line might be able to perform a similar function in the genome wide screen. Since the J-lat cell line produces GFP by the LTR-TAT expression system, host factors that affect LTR-TAT expression and not Env specifically would affect GFP signal in both cell lines, instead of only the EnvGFP-expressing cells.

Partial knockout of IFITM1 and GBP5 affects Env restriction by IFN

In further preparation for the genome wide KO screen, the LTR-TAT-driven EnvGFP-expressing Jurkat T-cells were transduced with lentiviral vectors introducing CRISPR-based knockouts against HIV-1 restriction factors IFITM1 and GBP5, after which expression was analysed by western blotting (*fig. 6*). Since no repetition experiments were performed, these data should be seen as preliminary. The basal expression levels of IFITM1 lied below the detection limit, making it impossible to judge the success of the knockout in the absence of IFN treatment (*fig. 6A*). The expression levels of IFITM1 protein upon interferon stimulation were only 16 and 26% lower than in the parent population, meaning IFITM1 was knocked out of an insufficient amount of cells to generate a KO cell line. In the two GBP5 knockout populations, basal GBP5 expression was lowered by 49% and 55% and interferon induced expression by 61 and 72%, respectively (*fig. 6B*). Interestingly, the restriction of Env expression by the interferon response was considerably weaker in the second GBP5 KO population than in the parent population (*fig. 6C*). To establish a cell line, single-cell clones can be generated from the GBP5 KO populations, after which genome sequencing can be used to assess whether knockout has been achieved in both alleles of the restriction factor genes. This KO cell line could subsequently be used to assess whether Env expression and localisation in the LTR-TAT EnvGFP Jurkat T-cell line are affected by a known restriction factor.

Conclusion

In this research, a Jurkat T derived cell line was generated expressing NL4.3 Env V5.3 GFP OPT by the authentic HIV-1 Tat-dependent LTR promoter. The generation of an EnvGFP-expressing cell line driven by CMV was not possible. Preliminary results show that the LTR-TAT driven cell line is reactivatable by Panobinostat, indicating that the cell line can serve as a model to study the expression of Env in latently infected cells. The degree of reactivation in the cells seems to be affected by the interferon response.

Overall, the creation of this cell line presents a powerful tool for research into HIV-1 Env. Firstly, the cells can be used to execute a genome wide screen to identify host factors that affect surface levels of Env during latency reversal. Characterisation of such host factors may contribute to the search for curative treatment for HIV-1 via the 'shock and kill' strategy. The generated cell line provides a more biologically relevant model for studying latent infection than the existing J-lat cell line, as it produces Env upon reactivation instead of a GFP surrogate. Other applications of the generated cell line may include studies into therapeutics that improve the surface presentation of Env during latency reversal.

Transduction of EnvGFP-expressing Jurkat T-cells with GBP5 lentiCRISPRv2 KO particles considerably reduced the basal and IFN-induced expression of GBP5. While repetition experiments are required to draw statistically relevant conclusions, the reduction in restriction factor expression seemed to weaken the restriction of Env expression by the interferon response. Further research is required to demonstrate that the created cell line can interact with known restriction factors.

Layman's abstract

To this day, no cure has been found for HIV. While the development of antiviral therapies have increased the lifespan of HIV patients considerably, not everybody has access to the permanent medical attention that treatment of an HIV infection requires. One reason that doctors have not been able find a cure for HIV, is that this virus is able to avoid detection by the immune system by developing latent or 'sleeping' infection in its host cells. The preferred target for HIV is the T-cell, a cell that lays dormant until the immune response is activated. Some activated T-cells survive their HIV infection long enough to revert back to a resting 'memory' state. While infected cells normally produce viral proteins in order to spread the infection to other cells, these sleeping T-cells do not, making them essentially invisible to the immune system.

An important target for scientists looking for a cure for HIV is the reactivation of latently infected cells. Clinical research has already shown that cells can be forced out of hiding using a category of drugs dubbed latency reversal agents. A key element of this so called 'shock and kill' strategy, is that reactivated cells are killed by the immune system. This decreases the amount of latently infected cells, eventually leading to the eradication of all infected cells in the patient. Detection of HIV infected cells relies in large part on one viral protein: the envelope glycoprotein or Env. Env is the only HIV protein that is presented on the cell surface during infection, making it a primary target for recognition by the immune system. This means that the surface presentation of Env in reactivating cells is essential to the 'shock and kill' strategy.

In this research, a cell line was created to serve as a model Env expression in cells carrying a latent HIV infection. The cell line produces Env fused with GFP, allowing the production and surface presentation of this essential protein to be tracked. Reactivation experiments showed that the production of Env could be induced by treatment of with a latency reversal agent, indicating that the cell line mimics the behaviour of latently infected cells. The cell line was further investigated by disabling genes from the host that are known to work against or 'restrict' the Env protein. Disabling one of these restriction factors (GBP5) affected the production of Env. This means that the cell line might be useful in the search for other genes that affect the surface presentation of Env during latency reversal, making it a powerful new tool in the search for a cure for HIV.

Bibliography

Abraham, R. T., & Weiss, A. (2004). Jurkat T cells and development of the T-cell receptor signalling paradigm. *Nature Reviews Immunology 2004 4:4*, *4*(4), 301–308. https://doi.org/10.1038/NRI1330

agilent.com. (2022). QuikChange II Site-Directed Mutagenesis Kit Instruction Manual. *Agilent Technologies, Inc* . https://www.agilent.com/cs/library/usermanuals/public/200523.pdf

Ait-Ammar, A., Kula, A., Darcis, G., Verdikt, R., de Wit, S., Gautier, V., Mallon, P. W. G., Marcello, A., Rohr, O., & van Lint, C. (2020). Current Status of Latency Reversing Agents Facing the Heterogeneity of HIV-1 Cellular and Tissue Reservoirs. *Frontiers in Microbiology*, *10*, 3060. https://doi.org/10.3389/FMICB.2019.03060/BIBTEX

Albert, J., Berglund, T., Gisslén, M., Gröön, P., Sönnerborg, A., Tegnell, A., Alexandersson, A., Berggren, I., Blaxhult, A., Brytting, M., Carlander, C., Carlson, J., Flamholc, L., Follin, P., Haggar, A., Hansdotter, F., Josephson, F., Karlström, O., Liljeros, F., … Widgren, K. (2014). Risk of HIV transmission from patients on antiretroviral therapy: A position statement from the Public Health Agency of Sweden and the Swedish Reference Group for Antiviral Therapy. *Scandinavian Journal of Infectious Diseases*, *46*(10), 673. https://doi.org/10.3109/00365548.2014.926565

Archin, N. M., Kirchherr, J. L., Sung, J. A. M., Clutton, G., Sholtis, K., Xu, Y., Allard, B., Stuelke, E., Kashuba, A. D., Kuruc, J. D., Eron, J., Gay, C. L., Goonetilleke, N., & Margolis, D. M. (2017). Interval dosing with the HDAC inhibitor vorinostat effectively reverses HIV latency. *The Journal of Clinical Investigation*, *127*(8), 3126–3135. https://doi.org/10.1172/JCI92684

assets.thermofisher.com. (2022). *Lipofectamine™ 3000 Reagent Protocol*. Thermo Fisher Scientific. https://assets.thermofisher.com/TFS-Assets/LSG/manuals/lipofectamine3000_protocol.pdf

Babu, H., Ambikan, A. T., Gabriel, E. E., Akusjärvi, S. S., Palaniappan, A. N., Sundaraj, V., Mupanni, N. R., Sperk, M., Cheedarla, N., Sridhar, R., Tripathy, S. P., Nowak, P., Hanna, L. E., & Neogi, U. (2019). Systemic inflammation and the increased risk of inflamm-aging and age-associated diseases in people living with HIV on long term suppressive antiretroviral therapy. *Frontiers in Immunology*, *10*(AUG), 1965. https://doi.org/10.3389/FIMMU.2019.01965/BIBTEX

Bai, Y., Soda, Y., Izawa, K., Tanabe, T., Kang, X., Tojo, A., Hoshino, H., Miyoshi, H., Asano, S., & Tani, K. (2003). Effective transduction and stable transgene expression in human blood cells by a third-generation lentiviral vector. *Gene Therapy 2003 10:17*, *10*(17), 1446–1457. https://doi.org/10.1038/SJ.GT.3302026

Barabona, G., Mahiti, M., Toyoda, M., Kamori, D., Masoud, S., Judicate, G. P., Sunguya, B., Lyamuya, E., & Ueno, T. (2021). Advanced baseline immunosuppression is associated with elevated levels of plasma markers of fungal translocation and inflammation in long-term treated HIV-infected Tanzanians. *AIDS Research and Therapy*, *18*(1), 1–10. https://doi.org/10.1186/S12981-021-00381-9/FIGURES/3

Battivelli, E., Dahabieh, M. S., Abdel-Mohsen, M., Svensson, J. P., da Silva, I. T., Cohn, L. B., Gramatica, A., Deeks, S., Greene, W. C., Pillai, S. K., & Verdin, E. (2018). Distinct chromatin functional states correlate with HIV latency reactivation in infected primary CD4+ T cells. *ELife*, *7*. https://doi.org/10.7554/ELIFE.34655

beckmancoulter.com. (2022). *agencourt AMPure XP Instructions For Use*. Beckman Coulter. https://www.beckmancoulter.com/wsrportal/techdocs?docname=B37419

Beitari, S., Wang, Y., Liu, S.-L., & Liang, C. (2019). HIV-1 Envelope Glycoprotein at the Interface of Host Restriction and Virus Evasion. *Viruses*, *11*(4), 311. https://doi.org/10.3390/v11040311

Brodin, J., Zanini, F., Thebo, L., Lanz, C., Bratt, G., Neher, R. A., & Albert, J. (2016). Establishment and stability of the latent HIV-1 DNA reservoir. *ELife*, *5*(November2016). https://doi.org/10.7554/ELIFE.18889

Cary, D. C., & Peterlin, B. M. (2018). Procyanidin trimer C1 reactivates latent HIV as a triple combination therapy with kansui and JQ1. *PLOS ONE*, *13*(11), e0208055. https://doi.org/10.1371/JOURNAL.PONE.0208055

Chen, H. C., Martinez, J. P., Zorita, E., Meyerhans, A., & Filion, G. J. (2016). Position effects influence HIV latency reversal. *Nature Structural & Molecular Biology 2016 24:1*, *24*(1), 47–54. https://doi.org/10.1038/nsmb.3328

Chomont, N., El-Far, M., Ancuta, P., Trautmann, L., Procopio, F. A., Yassine-Diab, B., Boucher, G., Boulassel, M. R., Ghattas, G., Brenchley, J. M., Schacker, T. W., Hill, B. J., Douek, D. C., Routy, J. P., Haddad, E. K., & Sékaly, R. P. (2009). HIV reservoir size and persistence are driven by T cell survival and homeostatic proliferation. *Nature Medicine 2009 15:8*, *15*(8), 893–900. https://doi.org/10.1038/NM.1972

Cohn, L. B., Chomont, N., Deeks, S. G., Biohub, C. Z., & Francisco, S. (2020). The Biology of the HIV-1 Latent Reservoir and Implications for Cure Strategies. *Cell Host & Microbe*, *27*(4), 519–530. https://doi.org/10.1016/J.CHOM.2020.03.014

Costin, J. M., Rausch, J. M., Garry, R. F., & Wimley, W. C. (2007). Viroporin potential of the lentivirus lytic peptide (LLP) domains of the HIV-1 gp41 protein. *Virology Journal*, *4*(1), 1–14. https://doi.org/10.1186/1743-422X-4-123/FIGURES/5

Coull, J. J., Romerio, F., Sun, J.-M., Volker, J. L., Galvin, K. M., Davie, J. R., Shi, Y., Hansen, U., & Margolis, D. M. (2000). The Human Factors YY1 and LSF Repress the Human Immunodeficiency Virus Type 1 Long Terminal Repeat via Recruitment of Histone Deacetylase 1. *Journal of Virology*, *74*(15), 6790. https://doi.org/10.1128/JVI.74.15.6790-6799.2000

Davey, R. T., Bhat, N., Yoder, C., Chun, T. W., Metcalf, J. A., Dewar, R., Natarajan, V., Lempicki, R. A., Adelsberger, J. W., Miller, K. D., Kovacs, J. A., Polis, M. A., Walker, R. E., Falloon, J., Masur, H., Gee, D., Baseler, M., Dimitrov, D. S., Fauci, A. S., & Lane, H. C. (1999). HIV-1 and T cell dynamics after interruption of highly active antiretroviral therapy (HAART) in patients with a history of sustained viral suppression. *Proceedings of the National Academy of Sciences of the United States of America*, *96*(26), 15109–15114. https://doi.org/10.1073/PNAS.96.26.15109/ASSET/0E24EDF1-020A-4896-954E-8A745E04FA24/ASSETS/GRAPHIC/PQ2694528007.JPEG

Davis, H. E., Morgan, J. R., & Yarmush, M. L. (2002). Polybrene increases retrovirus gene transfer efficiency by enhancing receptor-independent virus adsorption on target cell membranes. *Biophysical Chemistry*, *97*(2–3), 159–172. https://doi.org/10.1016/S0301-4622(02)00057-1

Deeks, S. G., Archin, N., Cannon, P., Collins, S., Brad Jones, R., W P Jong, M. A., Lambotte, O., Lamplough, R., Ndungu, T., Sugarman, J., Tiemessen, C. T., Vandekerckhove, L., Lewin, S. R., Deeks, S., Lewin, S., de Jong, M., Ndhlovu, Z., Chomont, N., Brumme, Z., … Nelson Kankaka, E. (2021). Research priorities for an HIV cure: International AIDS Society Global Scientific Strategy 2021. *Nature Medicine 2021 27:12*, *27*(12), 2085–2098. https://doi.org/10.1038/S41591-021-01590-5

Desplats, P., Dumaop, W., Smith, D., Adame, A., Everall, I., Letendre, S., Ellis, R., Cherner, M., Grant, I., & Masliah, E. (2013). Molecular and pathologic insights from latent HIV-1 infection in the human brain. *Neurology*, *80*(15), 1415. https://doi.org/10.1212/WNL.0B013E31828C2E9E

Egan, M. A., Carruth, L. M., Rowell, J. F., Yu, X., & Siliciano, R. F. (1996). Human immunodeficiency virus type 1 envelope protein endocytosis mediated by a highly conserved intrinsic internalization signal in the cytoplasmic domain of gp41 is suppressed in the presence of the Pr55gag precursor protein. *Journal of Virology*, *70*(10), 6547. https://doi.org/10.1128/JVI.70.10.6547-6556.1996

Elliott, J. H., McMahon, J. H., Chang, C. C., Lee, S. A., Hartogensis, W., Bumpus, N., Savic, R., Roney, J., Hoh, R., Solomon, A., Piatak, M., Gorelick, R. J., Lifson, J., Bacchetti, P., Deeks, S. G., & Lewin, S. R. (2015). Short-term administration of disulfiram for reversal of latent HIV infection: a phase 2 dose-escalation study. *The Lancet HIV*, *2*(12), e520–e529. https://doi.org/10.1016/S2352-3018(15)00226-X

Grau-Expósito, J., Luque-Ballesteros, L., Navarro, J., Curran, A., Burgos, J., Ribera, E., Torrella, A., Planas, B., Badía, R., Martin-Castillo, M., Fernández-Sojo, J., Genescà, M., Falcó, V., & Buzon, M. J. (2019). Latency reversal agents affect differently the latent reservoir present in distinct CD4+ T subpopulations. *PLOS Pathogens*, *15*(8), e1007991. https://doi.org/10.1371/JOURNAL.PPAT.1007991

Gutiérrez, C., Serrano-Villar, S., Madrid-Elena, N., Pérez-Eĺas, M. J., Martń, M. E., Barbas, C., Ruipérez, J., Muñoz, E., Muñoz-Fernández, M. A., Castor, T., & Moreno, S. (2016). Bryostatin-1 for latent virus reactivation in HIV-infected patients on antiretroviral therapy. *AIDS*, *30*(9), 1385–1392. https://doi.org/10.1097/QAD.0000000000001064

Halper-Stromberg, A., Lu, C. L., Klein, F., Horwitz, J. A., Bournazos, S., Nogueira, L., Eisenreich, T. R., Liu, C., Gazumyan, A., Schaefer, U., Furze, R. C., Seaman, M. S., Prinjha, R., Tarakhovsky, A., Ravetch, J. v., & Nussenzweig, M. C. (2014). Broadly neutralizing antibodies and viral inducers decrease rebound from HIV-1 latent reservoirs in humanized mice. *Cell*, *158*(5), 989–999. https://doi.org/10.1016/J.CELL.2014.07.043/ATTACHMENT/3DBDDF17-2259-4293-AC33-BC9E8A1D7EDB/MMC4.PDF

Hamer, D. (2005). Can HIV be Cured? Mechanisms of HIV Persistence and Strategies to Combat It. *Current HIV Research*, *2*(2), 99–111. https://doi.org/10.2174/1570162043484915

Hendricks, C. M., Cordeiro, T., Gomes, A. P., & Stevenson, M. (2021). The Interplay of HIV-1 and Macrophages in Viral Persistence. *Frontiers in Microbiology*, *12*. https://doi.org/10.3389/FMICB.2021.646447

Ho, D. D., Neumann, A. U., Perelson, A. S., Chen, W., Leonard, J. M., & Markowitz, M. (1995). Rapid turnover of plasma virions and CD4 lymphocytes in HIV-1 infection. *Nature 1995 373:6510*, *373*(6510), 123–126. https://doi.org/10.1038/373123A0

Holm, G. H., Zhang, C., Gorry, P. R., Peden, K., Schols, D., Clercq, E. de, & Gabuzda, D. (2004). Apoptosis of Bystander T Cells Induced by Human Immunodeficiency Virus Type 1 with Increased Envelope/Receptor Affinity and Coreceptor Binding Site Exposure. *Journal of Virology*, *78*(9), 4541. https://doi.org/10.1128/JVI.78.9.4541-4551.2004

Huang, H., Liu, S., Jean, M., Simpson, S., Huang, H., Merkley, M., Hayashi, T., Kong, W., Rodríguez-Sánchez, I., Zhang, X., Yosief, H. O., Miao, H., Que, J., Kobie, J. J., Bradner, J., Santoso, N. G., Zhang, W., & Zhu, J. (2017). A novel bromodomain inhibitor reverses HIV-1 latency through specific binding with BRD4 to promote Tat and P-TEFb association. *Frontiers in Microbiology*, *8*(JUN), 1035. https://doi.org/10.3389/FMICB.2017.01035/BIBTEX

international.neb.com. (2022). *Dephosphorylation of 5´-ends of DNA using Antarctic Phosphatase Protocol*. New England BioLabs Inc. https://international.neb.com/protocols/0001/01/01/vector-dephosphorylation-protocol

Jordan, A., Bisgrove, D., & Verdin, E. (2003). HIV reproducibly establishes a latent infection after acute infection of T cells in vitro. *The EMBO Journal*, *22*(8), 1868–1877. https://doi.org/10.1093/EMBOJ/CDG188

Kauder, S. E., Bosque, A., Lindqvist, A., Planelles, V., & Verdin, E. (2009). Epigenetic Regulation of HIV-1 Latency by Cytosine Methylation. *PLOS Pathogens*, *5*(6), e1000495. https://doi.org/10.1371/JOURNAL.PPAT.1000495

Khanal, S., Schank, M., el Gazzar, M., Moorman, J., & Yao, Z. (2021). HIV-1 Latency and Viral Reservoirs: Existing Reversal Approaches and Potential Technologies, Targets, and Pathways Involved in HIV Latency Studies. *Cells*, *10*(2), 1–23. https://doi.org/10.3390/CELLS10020475

Kim, J. T., Zhang, T. H., Carmona, C., Lee, B., Seet, C. S., Kostelny, M., Shah, N., Chen, H., Farrell, K., Soliman, M. S. A., Dimapasoc, M., Sinani, M., Blanco, K. Y. R., Bojorquez, D., Jiang, H., Shi, Y., Du, Y., Komarova, N. L., Wodarz, D., … Zack, J. A. (2022). Latency reversal plus natural killer cells diminish HIV reservoir in vivo. *Nature Communications 2022 13:1*, *13*(1), 1–14. https://doi.org/10.1038/S41467-021-27647-0

Kim, Y., Anderson, J. L., & Lewin, S. R. (2018). Getting the “Kill” into “Shock and Kill”: Strategies to Eliminate Latent HIV. *Cell Host & Microbe*, *23*(1), 14–26. https://doi.org/10.1016/J.CHOM.2017.12.004

Krapp, C., Hotter, D., Gawanbacht, A., McLaren, P. J., Kluge, S. F., Stürzel, C. M., Mack, K., Reith, E., Engelhart, S., Ciuffi, A., Hornung, V., Sauter, D., Telenti, A., & Kirchhoff, F. (2016). Guanylate Binding Protein (GBP) 5 Is an Interferon-Inducible Inhibitor of HIV-1 Infectivity. *Cell Host and Microbe*, *19*(4), 504–514. https://doi.org/10.1016/J.CHOM.2016.02.019/ATTACHMENT/E1561612-4494-41F4-AEE4-D11160B9B7E0/MMC1.PDF

Kula, A., Delacourt, N., Bouchat, S., Darcis, G., Avettand-Fenoel, V., Verdikt, R., Corazza, F., Necsoi, C., Vanhulle, C., Bendoumou, M., Burny, A., de Wit, S., Rouzioux, C., Rohr, O., & van Lint, C. (2019).

Heterogeneous HIV-1 Reactivation Patterns of Disulfiram and Combined Disulfiram+Romidepsin Treatments. *Journal of Acquired Immune Deficiency Syndromes (1999)*, *80*(5), 605–613. https://doi.org/10.1097/QAI.0000000000001958

Kuo, H. H., & Lichterfeld, M. (2018). Recent progress in understanding HIV reservoirs. *Current Opinion in HIV and AIDS*, *13*(2), 137. https://doi.org/10.1097/COH.0000000000000441

Lassen, K. G., Ramyar, K. X., Bailey, J. R., Zhou, Y., & Siliciano, R. F. (2006). Nuclear Retention of Multiply Spliced HIV-1 RNA in Resting CD4+ T Cells. *PLOS Pathogens*, *2*(7), e68. https://doi.org/10.1371/JOURNAL.PPAT.0020068

Lenasi, T., Contreras, X., & Peterlin, B. M. (2008). Transcriptional Interference Antagonizes Proviral Gene Expression to Promote HIV Latency. *Cell Host & Microbe*, *4*(2), 123. https://doi.org/10.1016/J.CHOM.2008.05.016

Leth, S., Schleimann, M. H., Nissen, S. K., Højen, J. F., Olesen, R., Graversen, M. E., Jørgensen, S., Kjær, A. S., Denton, P. W., Mørk, A., Sommerfelt, M. A., Krogsgaard, K., Østergaard, L., Rasmussen, T. A., Tolstrup, M., & Søgaard, O. S. (2016). Combined effect of Vacc-4x, recombinant human granulocyte macrophage colony-stimulating factor vaccination, and romidepsin on the HIV-1 reservoir (REDUC): a single-arm, phase 1B/2A trial. *The Lancet HIV*, *3*(10), e463–e472. https://doi.org/10.1016/S2352-3018(16)30055-8

Lint, C. van, Emiliani, S., Ott, M., & Verdin1, E. (1996). Transcriptional activation and chromatin remodeling of the HIV-1 promoter in response to histone acetylation. *The EMBO Journal*, *15*(5), 1112. /pmc/articles/PMC450009/?report=abstract

Liu, R., Simonetti, F. R., & Ho, Y. C. (2020). The forces driving clonal expansion of the HIV-1 latent reservoir. *Virology Journal 2020 17:1*, *17*(1), 1–13. https://doi.org/10.1186/S12985-019-1276-8

Lodermeyer, V., Suhr, K., Schrott, N., Kolbe, C., Stürzel, C. M., Krnavek, D., Münch, J., Dietz, C., Waldmann, T., Kirchhoff, F., & Goffinet, C. (2013). 90K, an interferon-stimulated gene product, reduces the infectivity of HIV-1. *Retrovirology*, *10*(1), 111. https://doi.org/10.1186/1742-4690-10-111

McCauley, S. M., Kim, K., Nowosielska, A., Dauphin, A., Yurkovetskiy, L., Diehl, W. E., & Luban, J. (2018). Intron-containing RNA from the HIV-1 provirus activates type I interferon and inflammatory cytokines. *Nature Communications 2018 9:1*, *9*(1), 1–10. https://doi.org/10.1038/s41467-018-07753-2

Mckeating, J. A., Mcknight, A., & Moore, J. P. (1991). Differential loss of envelope glycoprotein gp120 from virions of human immunodeficiency virus type 1 isolates: effects on infectivity and neutralization. *Journal of Virology*, *65*(2), 852. https://doi.org/10.1128/JVI.65.2.852-860.1991

Meås, H. Z., Haug, M., Beckwith, M. S., Louet, C., Ryan, L., Hu, Z., Landskron, J., Nordbø, S. A., Taskén, K., Yin, H., Damås, J. K., & Flo, T. H. (2020). Sensing of HIV-1 by TLR8 activates human T cells and reverses latency. *Nature Communications*, *11*(1). https://doi.org/10.1038/S41467-019-13837-4

Miyoshi, H., Takahashi, M., Gage, F. H., & Verma, I. M. (1997). Stable and efficient gene transfer into the retina using an HIV-based lentiviral vector. *Proceedings of the National Academy of Sciences of the United States of America*, *94*(19), 10319–10323. https://doi.org/10.1073/PNAS.94.19.10319

mn-net.com. (2022). *NucleoSpin ® Gel and PCR Clean-up User Manual*. Macherey-Nagel GmbH. https://www.mn-net.com/media/pdf/02/1a/74/Instruction-NucleoSpin-Gel-and-PCR-Clean-up.pdf

Nakane, S., Iwamoto, A., & Matsuda, Z. (2015). The V4 and V5 Variable Loops of HIV-1 Envelope Glycoprotein Are Tolerant to Insertion of Green Fluorescent Protein and Are Useful Targets for Labeling. *The Journal of Biological Chemistry*, *290*(24), 15279. https://doi.org/10.1074/JBC.M114.628610

OhAinle, M., Helms, L., Vermeire, J., Roesch, F., Humes, D., Basom, R., Delrow, J. J., Overbaugh, J., & Emerman, M. (2018). A virus-packageable CRISPR screen identifies host factors mediating interferon inhibition of HIV. *ELife*, *7*. https://doi.org/10.7554/ELIFE.39823

Oyaizu, N., Mccloskey, T. W., Than, S., Hu, R., Kalyanaraman, V. S., & Pahwa, S. (1994). Cross-linking of CD4 molecules upregulates Fas antigen expression in lymphocytes by inducing interferon-gamma and tumor necrosis factor- alpha secretion. *Blood*, *84*(8), 2622–2631. https://doi.org/10.1182/BLOOD.V84.8.2622.2622

Park, R. J., Wang, T., Koundakjian, D., Hultquist, J. F., Lamothe-Molina, P., Monel, B., Schumann, K., Yu, H., Krupzcak, K. M., Garcia-Beltran, W., Piechocka-Trocha, A., Krogan, N. J., Marson, A., Sabatini, D. M., Lander, E. S., Hacohen, N., & Walker, B. D. (2016). A genome-wide CRISPR screen identifies a restricted set of HIV host dependency factors. *Nature Genetics 2016 49:2*, *49*(2), 193–203. https://doi.org/10.1038/NG.3741

Pinkevych, M., Cromer, D., Tolstrup, M., Grimm, A. J., Cooper, D. A., Lewin, S. R., Søgaard, O. S., Rasmussen, T. A., Kent, S. J., Kelleher, A. D., & Davenport, M. P. (2015). HIV Reactivation from Latency after Treatment Interruption Occurs on Average Every 5-8 Days—Implications for HIV Remission. *PLoS Pathogens*, *11*(7), Nature. https://doi.org/10.1371/JOURNAL.PPAT.1005000

qiagen.com. (2022a). *QIAprep® Miniprep Handbook*. QIAGEN. https://www.qiagen.com/us/resources/download.aspx?id=22df6325-9579-4aa0-819c-788f73d81a09&lang=en

qiagen.com. (2022b). *RNeasy Mini Handbook*. QIAGEN. https://www.qiagen.com/us/resources/download.aspx?id=14e7cf6e-521a-4cf7-8cbc-bf9f6fa33e24&lang=en

Rasmussen, T. A., Tolstrup, M., Brinkmann, C. R., Olesen, R., Erikstrup, C., Solomon, A., Winckelmann, A., Palmer, S., Dinarello, C., Buzon, M., Lichterfeld, M., Lewin, S. R., Ostergaard, L., & Søgaard, O. S. (2014). Panobinostat, a histone deacetylase inhibitor, for latent-virus reactivation in HIV-infected patients on suppressive antiretroviral therapy: a phase 1/2, single group, clinical trial. *The Lancet HIV*, *1*(1), e13–e21. https://doi.org/10.1016/S2352-3018(14)70014-1

Reeves, D. B., Duke, E. R., Wagner, T. A., Palmer, S. E., Spivak, A. M., & Schiffer, J. T. (2018). A majority of HIV persistence during antiretroviral therapy is due to infected cell proliferation. *Nature Communications 2018 9:1*, *9*(1), 1–16. https://doi.org/10.1038/S41467-018-06843-5

Rowell, J. F., Ruff, A. L., Guarnieri, F. G., Staveley-O'Carroll, K., Lin, X., Tang, J., August, J. T., & Siliciano, R. F. (1995). Lysosome-associated membrane protein-1-mediated targeting of the HIV-1 envelope protein to an endosomal/lysosomal compartment enhances its presentation to MHC class II-restricted T cells. *The Journal of Immunology*, *155*(4).

Sanjana, N. E., Shalem, O., & Zhang, F. (2014). Improved vectors and genome-wide libraries for CRISPR screening. *Nature Methods*, *11*(8), 783. https://doi.org/10.1038/NMETH.3047

Schneider, J., Kaaden, O., Copeland, T. D., Oroszlan, S., & Hunsmann, G. (1986). Shedding and interspecies type sero-reactivity of the envelope glycopolypeptide gp120 of the human immunodeficiency virus. *Journal of General Virology*, *67*(11), 2533–2538. https://doi.org/10.1099/0022-1317-67-11-2533/CITE/REFWORKS

Siliciano, J. D., Kajdas, J., Finzi, D., Quinn, T. C., Chadwick, K., Margolick, J. B., Kovacs, C., Gange, S. J., & Siliciano, R. F. (2003). Long-term follow-up studies confirm the stability of the latent reservoir for HIV-1 in resting CD4+ T cells. *Nature Medicine 2003 9:6*, *9*(6), 727–728. https://doi.org/10.1038/NM880

Siliciano, R. F., & Greene, W. C. (2011). HIV Latency. *Cold Spring Harbor Perspectives in Medicine:*, *1*(1). https://doi.org/10.1101/CSHPERSPECT.A007096

Søgaard, O. S., Graversen, M. E., Leth, S., Olesen, R., Brinkmann, C. R., Nissen, S. K., Kjaer, A. S., Schleimann, M. H., Denton, P. W., Hey-Cunningham, W. J., Koelsch, K. K., Pantaleo, G., Krogsgaard, K., Sommerfelt, M., Fromentin, R., Chomont, N., Rasmussen, T. A., Østergaard, L., & Tolstrup, M. (2015). The Depsipeptide Romidepsin Reverses HIV-1 Latency In Vivo. *PLoS Pathogens*, *11*(9). https://doi.org/10.1371/JOURNAL.PPAT.1005142

Spivak, A. M., Bosque, A., Balch, A. H., Smyth, D., Martins, L., & Planelles, V. (2015). Ex vivo bioactivity and HIV-1 latency reversal by ingenol dibenzoate and panobinostat in resting CD4+ T cells from aviremic patients. *Antimicrobial Agents and Chemotherapy*, *59*(10), 5984–5991. https://doi.org/10.1128/AAC.01077-15/ASSET/144E96D2-3FD2-41C4-ACD7-E98764554282/ASSETS/GRAPHIC/ZAC0091543800004.JPEG

Surre, J., Saint-Ruf, C., Collin, V., Orenga, S., Ramjeet, M., & Matic, I. (2018). Strong increase in the autofluorescence of cells signals struggle for survival. *Scientific Reports 2018 8:1*, *8*(1), 1–14. https://doi.org/10.1038/S41598-018-30623-2

Tada, T., Zhang, Y., Koyama, T., Tobiume, M., Tsunetsugu-Yokota, Y., Yamaoka, S., Fujita, H., & Tokunaga, K. (2015). MARCH8 inhibits HIV-1 infection by reducing virion incorporation of envelope glycoproteins. *Nature Medicine 2015 21:12*, *21*(12), 1502–1507. https://doi.org/10.1038/NM.3956

takarabio.com. (2022a). *CalPhos™ Mammalian Transfection Kit User Manual*. Takara Bio, Inc. https://www.takarabio.com/documents/User%20Manual/CalPhos%20Mammalian%20Transfection%20Kit%20User%20Manual_PT3025/CalPhos%20Mammalian%20Transfection%20Kit%20User%20Manual_PT3025-1_062013.pdf

takarabio.com. (2022b). *In-Fusion® Snap Assembly User Manual*. Takara Bio, Inc. https://www.takarabio.com/documents/User%20Manual/In/In-Fusion%20Snap%20Assembly%20User%20Manual.pdf

thermofisher.com. (2022a). *MAX Efficiency® Stbl2™ Competent Cells*. Thermo Fisher Scientific. https://www.thermofisher.com/document-connect/document-connect.html?url=https%3A%2F%2Fassets.thermofisher.com%2FTFS-Assets%2FLSG%2Fmanuals%2FMaxEfficiency_stbl2_man.pdf

thermofisher.com. (2022b). *Rat IgG2a kappa Isotype Control, eFluor™ 660*. Thermo Fisher Scientific. https://www.thermofisher.com/antibody/product/Rat-IgG2a-kappa-clone-eBR2a-Isotype-Control/50-4321-82

tools.thermofisher.com. (2022). *DNA Insert Ligation (sticky-end and blunt-end) into Vector DNA Protocol*. Thermo Fisher Scientific. https://tools.thermofisher.com/content/sfs/manuals/MAN0011906_DNAsert_Ligation_Vector_DNA_UG.pdf

Tyagi, M., & Karn, J. (2007). CBF-1 promotes transcriptional silencing during the establishment of HIV-1 latency. *The EMBO Journal*, *26*(24), 4985. https://doi.org/10.1038/SJ.EMBOJ.7601928

van der Sluis, R. M., Kumar, N. A., Evans, V. A., Dantanarayana, A. I., Sékaly, R. P., Fromentin, R., Chomont, N., Cameron, P. U., & Lewin, S. R. (2017). OA3-3 Anti-PD-1 disrupts HIV latency in non-proliferating but not in proliferating T cells. *Journal of Virus Eradication*, *3*, 4. https://doi.org/10.1016/S2055-6640(20)30840-2

Wei, X., Ghosh, S. K., Taylor, M. E., Johnson, V. A., Emini, E. A., Deutsch, P., Lifson, J. D., Bonhoeffer, S., Nowak, M. A., Hahn, B. H., Saag, M. S., & Shaw, G. M. (1995). Viral dynamics in human immunodeficiency virus type 1 infection. *Nature 1995 373:6510*, *373*(6510), 117–122. https://doi.org/10.1038/373117A0

Wightman, F., Solomon, A., Kumar, S. S., Urriola, N., Gallagher, K., Hiener, B., Palmer, S., McNeil, C., Garsia, R., & Lewin, S. R. (2015). Effect of ipilimumab on the HIV reservoir in an HIV-infected individual with metastatic melanoma. *AIDS (London, England)*, *29*(4), 504. https://doi.org/10.1097/QAD.0000000000000562

Williams, S. A., Chen, L. F., Kwon, H., Ruiz-Jarabo, C. M., Verdin, E., & Greene, W. C. (2006). NF-κB p50 promotes HIV latency through HDAC recruitment and repression of transcriptional initiation. *The EMBO Journal*, *25*(1), 139. https://doi.org/10.1038/SJ.EMBOJ.7600900

Yu, J., Li, M., Wilkins, J., Ding, S., Swartz, T. H., Esposito, A. M., Zheng, Y. M., Freed, E. O., Liang, C., Chen, B. K., & Liu, S. L. (2015). IFITM Proteins Restrict HIV-1 Infection by Antagonizing the Envelope Glycoprotein. *Cell Reports*, *13*(1), 145. https://doi.org/10.1016/J.CELREP.2015.08.055

Zhou, T., Dang, Y., & Zheng, Y.-H. (2014). The Mitochondrial Translocator Protein, TSPO, Inhibits HIV-1 Envelope Glycoprotein Biosynthesis via the Endoplasmic Reticulum-Associated Protein Degradation Pathway. *Journal of Virology*, *88*(6), 3474. https://doi.org/10.1128/JVI.03286-13

Zhou, T., Frabutt, D. A., Moremen, K. W., & Zheng, Y. H. (2015). ERManI (Endoplasmic Reticulum Class I α-Mannosidase) Is Required for HIV-1 Envelope Glycoprotein Degradation via Endoplasmic Reticulum-associated Protein Degradation Pathway. *The Journal of Biological Chemistry*, *290*(36), 22184. https://doi.org/10.1074/JBC.M115.675207

Experimental Method

Supplementary table 1 provides a list of equipment and materials that were used.

Cell culture

Human embryonic kidney (HEK) 293T cells, a cell line stably expressing simian virus 40 T-antigen, were cultured in Delbucco's modified Eagle's medium (DMEM), supplemented with 1% penicillin-streptomycin (pen-strep), 2 mM L-Glutamine and 10% fetal calf/bovine serum (FCS). Hereafter this medium is referred to as DMEM. Jurkat leukemic T-cells and J-lat cells were cultured in RPMI-1640 medium, supplemented with 1% pen-strep, 2 mM L-Glutamine, 10% FCS, 1% MEM Non-Essential Amino Acids and 1 mM sodium pyruvate (Abraham & Weiss, 2004). This medium is hereafter referred to as RPMI. The J-lat cell line is a derivative of the Jurkat T-cell, engineered to express GFP driven by the LTR-TAT expression system native to HIV-1 (Jordan et al., 2003). All subclones generated from Jurkat T-cells in this study are cultured in the same manner as the parental cell line.

Construction of lentiviral expression vectors

Molecular cloning of LTR-TAT- and CMV-driven EnvGFP expression vectors

A plasmid carrying the NL4.3 Env gene with GFP OPT inserted in the V5.3 variable loop was created by D. Postmus by cloning GFP OPT into the full length pNL4.3 plasmid (McCauley et al., 2018). The EnvGFP gene was amplified by a polymerase chain reaction (PCR). Primers were used with overhangs containing a *Eco*RI restriction site for insertion of EnvGFP into the the pHR' CMV lentiviral vector (Miyoshi et al., 1997) or a *Msc*I restriction site for its insertion in the the LTR-TAT-driven lentiviral vector (Jordan et al., 2003). The following ingredients were used for the insert amplifications: 1x Q5 reaction buffer, 200 µM dNTPs, 500 nM forward and reverse primer, 0.02 U/µL Q5 polymerase, 1x GC enhancer, nuclease-free H_2O and 0.2-2.0 ng/µL NL4.3 Env V5.3 GFP OPT plasmid. Primers F3 and R4, and primers F1 and R2 (*supplementary table 2*) were used for the CMV insert and for the LTR-TAT insert, respectively). The PCR protocol was as follows: 0:30 98°C, 40 x (0:10 98°C, 0:30 65/67/69°C, 1:00 72°C), 2:00 72°C. The annealing temperature and template concentration were varied in an effort to achieve optimal yield and product specificity. The PCR product was loaded on a 0.7% agarose DNA gel (100-120 V, 90 min). Since no nonspecific side products were found, the CMV insert was obtained directly from the PCR product by purification using the NucleoSpin Gel and PCR Clean-up kit (mn-net.com, 2022). For the LTR-TAT insert, bands were excised from the gel and the DNA was purified from the gel using NucleoSpin Gel and PCR Clean-up kit. The CMV insert was digested overnight at 37°C in 1x rCutSmart™ buffer with 8 U *Xho*I and *Eco*RI-HF per µg of DNA. Digestion of the LTR-TAT insert was performed in the same manner, with 20 U *Xho*I per µg of DNA. A PCR cleanup was performed after digestion. The pHR' CMV backbone was digested with 8 U *Xho*I and *Eco*RI per µg of DNA and dephosphorylated by Antarctic Phosphatase by the provided protocol to prevent religation (international.neb.com, 2022). The digestion product was electrophoresed on a 0.7% agarose DNA gel (80-120 V, 75 min), excised from the gel and purified. The lentiviral backbone containing LTR-TAT was digested using 8 U *Xho*I and *Msc*I per µg of DNA, dephosphorylated and gel-purified.

The EnvGFP gene insert was inserted into the lentiviral vectors carrying the CMV and LTR promoters through ligation by the T4 DNA Ligase and subsequently transformed into Stbl2™ Competent Cells according to the recommended protocols (thermofisher.com, 2022a; tools.thermofisher.com, 2022). Insert to vector ratios between 3:1 and 20:1 were used in parallel to maximise the chances of a successful ligation. 1 to 5 µL of undiluted ligation mix, or alternatively 1 µL of 5x diluted ligation mix were used for

transformation. The transformed bacteria were plated on Terrific Broth (LB) medium with 50 µg/mL ampicillin. Plasmid was extracted from the bacteria using the QIAprep Spin Miniprep Kit (qiagen.com, 2022a), digested using *Xho*I and *Eco*RI (CMV-EnvGFP) or *Xho*I and *Msc*I (LTR-TAT-EnvGFP) and ran on a 1% agarose DNA gel (80 V, 60 min) to validate the ligation. Sanger sequencing was used to check for mutations potentially introduced during the PCR-based cloning process.

In order to insert a kozak sequence in front of the starting codon for Env, the CMV-EnvGFP plasmid was amplified using primers F13 and R14 (*supplementary table 2*) using the QuikChange Site-Directed Mutagenesis Kit and transformed into XL1-Blue Supercompetent cells according to the provided protocol (agilent.com, 2022).

InFusion cloning of LTR-TAT-driven EnvGFP expression vector

The NL4.3 Env V5.3 GFP OPT plasmid was amplified using primers with overhangs complementary to the lentiviral vector containing the LTR-TAT expression system, in preparation for an InFusion cloning reaction. The amplification was performed with primers F7 and R8 (*supplementary table 2*), in combination with the following ingredients: 1x Q5 reaction buffer, 200 µM dNTPs, 500 nM forward and reverse primer, 0.02 U/µL Q5 polymerase, 1x GC enhancer, nuclease-free H_2O and 1.0 ng/µL NL4.3 Env V5.3 GFP OPT plasmid. PCR protocol: 0:30 98°C, 1 x (0:10 98°C, 0:30 66°C, 1:00 72°C), 40 x (0:10 98°C, 0:30 70°C, 1:00 72°C), 2:00 72°C. The PCR product was separated on a 0.7% agarose DNA gel (100-120 V, 90 min), bands were excised and DNA was purified from the gel. The LTR-TAT-driven lentiviral vector was amplified by inverse PCR using primers F5 and R6 (*supplementary table 2*) to obtain the backbone. The following ingredients were used: 1x Q5 reaction buffer, 200 µM dNTPs, 500 nM forward and reverse primer, 0.02 U/µL Q5 polymerase, 1x GC enhancer, nuclease-free H_2O and 0.2-1.0 ng/µL NL4.3 Env V5.3 GFP OPT plasmid. The PCR protocol was as follows: 0:30 98°C, 40 x (0:10 98°C, 0:30 69/71/73°C, 1:00 72°C), 2:00 72°C. The annealing temperature and template concentration were varied to achieve optimal product yield and specificity. To concentrate the product of the PCR, 800 µL of PCR product was precipitated by adding 0.6x isopropanol, followed by centrifugation (20 min, 15,000 *g*, 4°C). The pellet was washed in 1x ethanol, centrifuged again, air dried and resuspended in 200 µL TE (pH 8.0) buffer. The concentrated DNA was run on a 0.7% agarose DNA gel, bands were excised and DNA was purified from the gel. A paramagnetic bead-based PCR clean-up kit (AMPure XP for PCR Purification) was used to improve the purity of the PCR product further (beckmancoulter.com, 2022). The insert and backbone were ligated using 1x In-Fusion HD Enzyme Premix according to the provided protocol (takarabio.com, 2022b). 2.5 to 5 µL of undiluted ligation mix, or alternatively 5 µL of 5x diluted ligation mix were used for transformation into Stbl2™ Competent Cells. Transformed cells were plated on TB medium with 1 µg/µL ampicillin, after which DNA was extracted from the bacteria using the QIAprep Spin Miniprep Kit (qiagen.com, 2022a). To validate the ligation, the plasmid was digested by *Xho*I and *Msc*I and ran on a 0.7% agarose DNA gel (100-120 V, 60 min) to validate the ligation. Sanger sequencing was used to confirm that no mutations were introduced during the cloning process. The resulting plasmid was digested with 8 U *Msc*I per µg of DNA, gel purified and re-ligated using T4 DNA Ligase, followed by transformation, antibiotic selection and DNA extraction as described above.

Trial transfections

The EnvGFP expression of the created plasmids was determined by transfection into HEK293T cells. 150,000 cells were seeded in a 24-well format and cultured overnight at 37°C. At 70% confluence, the cells were transfected with 500 ng DNA using Lipofectamine 3000 according to the provided protocol (assets.thermofisher.com, 2022). The parent plasmids (pHR' CMV-GFP and the LTR-TAT GFP expression vector) and a CMV-driven HXB2 Env V5.3 GFP OPT expression plasmid (Nakane et al., 2015) were

transfected in parallel to the cloned plasmids. After 20 to 24 hours, the cells were harvested, surface-stained with α-GFP eF660 and analysed by flow cytometry using the BD FACSCelesta™ Cell Analyzer.

Flow cytometry

To prepare HEK293T cells for flow cytometric analysis, cells were washed with 1x phosphate buffer saline (PBS), trypsinised and resuspended in 1x DMEM. The cells were pelleted (300 *g*, 5 min, RT), washed with 1x PBS, pelleted again and fixed by resuspension in paraformaldehyde (PFA). Cells from the 'infectious cell culture'-lab, where use of pseudoparticles is permitted, were fixed using 4% PFA, other cells were fixed using 2% PFA. Cells were kept on ice until fixing. Suspension cells were pelleted (400 *g*, 5 min, RT), washed with 1x PBS, pelleted again and fixed by resuspension in PFA.

To apply α-GFP surface staining, cells were washed with 1x FACS buffer (1x PBS, 1% bovine serum albumin (BSA), 0.1% sodium azide, sterile filtered) after the first centrifugation step, pelleted and resuspended in 1:300 α-GFP eF660 APC antibody solution. After 20 min incubation at 4°C, the cells were diluted by 1x FACS buffer, washed with 1x FACS buffer and fixed by resuspension in PFA. Unstained control cells were incubated in FACS buffer instead of antibody solution. For α-Env surface staining, cells were incubated in 5 µg/mL α-Env 2G12 primary antibody solution for 30 min at 4°C, washed with 1x PBS and subsequently incubated in 1:100 α-human AF633 secondary antibody solution for 3o min at 4°C. Cells were washed in PBS and fixed by resuspension in PFA. A secondary-antibody-only control was prepared by incubating cells in PBS instead of primary antibody.

Fixed cells were analysed in the BD FACSCelesta™ Cell Analyzer, after which data is processed using the BD FACSDiva™ software.

Generation of EnvGFP-expressing Jurkat T-cell line by transduction

VSV-G-pseudotyped lentiviral particles were generated by co-transfection of three plasmids into HEK293T cells, as described in (Bai et al., 2003). Either the LTR-TAT- or CMV-driven EnvGFP plasmid was transfected as transfer plasmid. Alongside the transfer plasmid, a plasmid containing the gene for the VSV-G protein and a pCMV packaging plasmid containing the gag-pol genes were used. Transfection was performed using a calcium phosphate transfection kit according to the provided protocol (takarabio.com, 2022a). The medium on the transfected cells was replaced with fresh medium 16 h after transfection. 48 and 72 h after transfection, viral supernatants were harvested, filtered through membranes with 45 µm pore size and concentrated by ultracentrifugation (30,000 rpm, 1 h, 4°C) using a 20% sucrose cushion. The pellet was resuspended in DMEM, concentrating the lentiviral particles 100-fold. Viral stocks were aliquoted and stored at -80°C.

Jurkat T-cells were transduced with lentiviral particles by spinoculation. To this end, 1 million cells/mL are seeded in RPMI and incubated at 37°C, 5% CO_2 for 4 h. After, lentiviral particles containing either the LTR-TAT- or CMV-EnvGFP transfer plasmids were added to the cells in a 1:100, 1:10, 1:2 and 1:1 volume/volume ratio in the presence and absence of 8 µg/mL polybrene. The mix is centrifuged at (400 *g*, 1:30 h, RT). After transduction, the cells were cultured in RPMI. One day after transduction, the cells were pelleted (400 *g*, 5 min) and imaged using the DMi8 S Platform Live-Cell-Microscope. Five days after transduction, a fraction of the transduced cells was used for flow cytometric analysis. Eight days after transduction, the two populations of Jurkat T-cells transduced with the LTR-TAT EnvGFP vector and one with CMV-EnvGFP were enriched for GFP-positive cells by fluorescence-activated cell sorting (FACS). 4800 LTR-TAT EnvGFP cells were deposited into one well, creating a bulk population of GFP-positive cells.

Besides, 196 cells were individually deposited into separate wells. These cells will hereafter be referred to as single-cell clones. From the cells transduced with the CMV-EnvGFP vector, twelve wells were filled with a single GFP-positive cell and twelve wells were filled with three, five and ten cells. The latter are hereafter referred to as multiple cell clones. The sorted cells are cultured in RPMI and routinely checked for viability using light microscopy. The LTR-TAT EnvGFP bulk population, seven single-cell clones and four CMV-EnvGFP multiple cell clones were expanded for further characterisation.

Reactivation of Jurkat T-cells

The transduced Jurkat T-cells obtained by cell sorting were reactivated by Panobinostat and analysed using flow cytometry, western blot and RT-qPCR. Cells were seeded in RPMI at 1 million cells/mL for a readout by flow cytometry and at 2 m cells/mL for western blot and RT-PCR. After 4 h of incubation at 37°C, 5% CO_2, the cells were incubated with 50 mM Panobinostat at 37°C, 5% CO_2 for 24 h. Cells were harvested for flow cytometric analysis and surface-stained with α-GFP or α-Env antibodies as described previously. For western blot analysis, reactivated cells were pelleted (400 *g*, 5 min), washed in 1x PBS, resuspended in 40 µL M-PER™ Mammalian Protein Extraction Reagent and incubated for 20 min at 4°C. Then, the cells were centrifuged (17,900 *g*, 10 min, 4°C), after which the supernatant was combined with 1x SDS buffer and boiled at 95°C for 5 min. Samples are separated by sodium dodecyl sulphate polyacrylamide gel electrophoresis (SDS-PAGE), transferred onto a membrane and incubated with α-Env and α-GAPDH antibodies. A detailed description of the western blot analysis is provided in the section below.

To prepare samples for analysis by RT-qPCR, RNA was extracted from reactivated cells using the Qiagen RNeasy® Mini Kit according to the provided protocol (qiagen.com, 2022b). During the RNA extraction, on column DNase digestion was performed. Per sample, aliquots of 10 µL RNA were combined with 1 µL dNTP (10 mM), 1 µL random hexamers (100 µM) and 4 µL nuclease-free H_2O in duplicate, incubated at 75°C for 3 min and put on ice. One aliquot is then combined with 2 µL 10x reverse transcriptase (RT) reaction buffer, 1.5 µL H_2O and 0.5 µL M-MuLV RT. In the second aliquot, 2 µL H_2O and no RT is used. The samples were incubated at 42°C for 1 h and at 90°C for 10 min. RT-qPCR was performed using the Roche LightCycler® 480 II with primers and probes against NL4.3 Env and RNase P. The following ingredients were used: 1 µL forward Env primer (10 µM), 1 µL reverse Env primer (10 µM), 0.3 µL Env probe (10 µM), 1 µL of RNase P primer probe, 10 µL of LightCycler® 480 Probes Master Mix, 4.7 µL H_2O and 2 µL of cDNA template (see *supplementary table 2* for the primer and probe sequences). The PCR protocol was as follows: 2:00 50°C, 10:00 98°C, 40 x (0:15 95°C, 1:00 60°C), 0:30 37°C. Fluorescence of the probes was acquired at 465-510 nm and 533-580 nm.

In another experiment, the transduced Jurkat T-cells were pre-treated with 250 IU/mL IFN-α-2a before reactivation as described above. After reactivation, intact cells were surface-stained with α-GFP eF660 and analysed by flow cytometry. The MFI of the IFN-treated, reactivated cells was corrected for the difference in fluorescence between the mock-treated and IFN-only control: $MFI_{corrected} = MFI_{IFN+pano} * MFI_{mock} / MFI_{IFN}$.

Western blot analysis

Samples were combined 1:3 with 4x SDS reducing buffer and boiled at 95°C for 10 min. All samples were loaded onto 10% handcast SDS gels and run for 10 minutes at 80 V and 80 minutes at 100 V. SDS gels were transferred onto PVDF membranes using the Bio-Rad Trans Blot Turbo transfer system. The membranes were blocked with blocking buffer (1x PBS, 5% skim milk) for 2 h at room temperature and incubated

overnight with primary antibody with 1x PBS, 1% BSA and 0.05% sodium-azide at 4°C. The following primary antibodies were used: 1:1000 rabbit α-gp120, 1:5000 mouse α-IFITM1, 1:1000 rabbit α-GBP5 and 1:1000 mouse α-GAPDH (see *supplementary table 1* for detailed product specifications). The membranes were washed 4 times (for 1, 2, 12 and 15 min) with PBS-T (1x PBS, 0.1% Tween-20) and incubated for 1 h with secondary antibody with TBS-T (1x TBS, 0.1% Tween-20) and 1% milk at room temperature. Either 1:10000 donkey α-rabbit 800CW or 1:10000 goat α-mouse 800CW were used as secondary antibody. The membranes were washed four times (for 1, 2, 12 and 15 min) with PBS-T and imaged using with the LI-COR Odyssey® CLx Imaging System.

Knock out of *IFITM1* and *GBP5* in Jurkat T-cells

VSV-G-pseudotyped lentiviral particles were generated as described previously, in this case carrying a lentiCRISPRv2 transfer plasmid for CRISPR-based knockout (KO) by transduction (Sanjana et al., 2014). This plasmid contains genes for a Cas9 nuclease and single guide RNA (sgRNA) sequences targeting either *IFITM1* or *GBP5*, accompanied by a puromycin resistance-conferring gene. The bulk population of LTR-TAT EnvGFP Jurkat T-cells was transduced by the *IFITM1* and *GBP5* KO particles by spinoculation as described previously. After transduction, the cells cultured in RPMI containing 1 µg/mL puromycin. 20 days after transduction, two transduced populations for each KO were harvested and analysed by western blot. Half of the cells were treated for 24 h with 250 IU/mL interferon-α-2a before harvest, the other half was mock-treated. Primary antibodies against IFITM1 and GBP5, gp120 and GAPDH were used.

Supplementary

Supplementary table 1: *list of equipment and materials used in this research.*

SDS-Page, western blot	
Rotiphorese® Gel 30% (37,5:1)	Carl Roth #3029
TEMED (Electrophoresis)	Thermo Fisher Scientific #BP150-20
NuPAGE™ MES SDS Running Buffer (20X)	Thermo Fisher Scientific #NP0002
PowerPac™ HC High-Current Power Supply	Bio-Rad Laboratories, Inc. #1645052
ChemiDoc XRS+ System	Bio-Rad Laboratories, Inc. #1708265
Trans-Blot Turbo Transfer System	Bio-Rad Laboratories, Inc. #1704150
Odyssey® CLx Imaging System	LI-COR Biosciences - GmbH #976-12809
Monoclonal Mouse anti-IFITM1 IgG2a Antibody	Proteintech Group, Inc. #60074-1lg
Monoclonal Rabbit anti-GBP5 IgG Antibody (D3A5O)	Cell Signaling Technology, Inc. #67798
Polyclonal Rabbit anti-gp120 Antibody	(Lodermeyer et al., 2013), gift from Valerie Bosch
Polyclonal Rabbit anti-Tubulin Antibody	Cell Signaling Technology, Inc. #2144
Monoclonal Mouse anti-GAPDH IgM Antibody (1D4)	Novus Biologicals #NB300-221
IRDye® 800CW Donkey anti-Rabbit IgG Secondary Antibody	LI-COR Biosciences, GmbH #926-32213
IRDye® 800CW Goat anti-Mouse IgG Secondary Antibody	LI-COR Biosciences, GmbH #926-32210
IRDye® 680LT Goat anti-Rabbit IgG Secondary Antibody	LI-COR Biosciences, GmbH #926-68021

Cloning	
pHR' CMV GFP plasmid	Addgene #14858, gift from Inder Verma
LTR-TAT GFP plasmid	(Jordan et al., 2003), gift from Albert Jordan
pNL4.3 plasmid	Addgene #101341, gift from Jeremy Luban
ThermoMixer© F1.5	Eppendorf SE #5384000012
*Xho*I	New England BioLabs, Inc. #R0146
*Eco*RI-HF®	New England BioLabs, Inc. #R3101

*Msc*I	New England BioLabs, Inc. #R0534
rCutSmart™ Buffer	New England BioLabs, Inc. #B6004
Antarctic Phosphatase	New England BioLabs, Inc. #M0289
Mastercycler® nexus gradient - PCR Thermocycler	Eppendorf SE #6331000017
NucleoSpin Gel and PCR Clean-up kit	Macherey-Nagel GmbH #740609.50
Q5® High-Fidelity DNA Polymerase	New England BioLabs, Inc. #M0491
NanoDrop™ One	Thermo Fischer Scientific #ND-ONE-W
Max Efficiency® Stbl2™ Competent Cells	Thermo Fisher Scientific #10268019
S.O.C. medium	Thermo Fisher Scientific #15544034
QIAprep Spin Miniprep Kit	Qiagen #27106X4
T4 DNA Ligase	Thermo Fisher Scientific #EL0011
In-Fusion® HD Cloning Plus kit	Takara Bio Inc. #638909
QuikChange Site-Directed Mutagenesis Kit	Agilent Technologies, Inc #200518

Cell culture, transient expression and particle generation

DMEM Medium	Merck KGaA #D5796
RPMI-1640 Medium	Merck KGaA #R8758
Mr. Frosty™ Freezing Container	Thermo Fisher Scientific #5100-0001
MEM Non-Essential Amino Acids (100x)	Thermo Fisher Scientific #11140050
M-PER™ Mammalian Protein Extraction Reagent	Thermo Fisher Scientific #78501
TC20 Automated Cell Counter	Bio-Rad Laboratories, Inc. # 1450102
Lipofectamine™ 2000 Transfection Reagent	Thermo Fisher Scientific #11668027
Lipofectamine™ 3000 Transfection Reagent	Thermo Fisher Scientific #L3000001
Lipofectamine™ LTX Reagent with Plus Reagent	Thermo Fisher Scientific #15338030
Opti-MEM™ Serum Reduced Medium	Thermo Fisher Scientific #31985070
CalPhos™ Mammalian Transfection Kit	Takara Bio Inc. #631312
Optima™ L-90K Ultracentrifuge	Beckman Coulter #8043-30-1191
A27-8x50 Fixed Angle Rotor	Thermo Fisher Scientific #75003008

Microscopy and flow cytometry, qPCR

DMi8 S Platform Live-Cell-Microscope	Leica Microsystems
µ-Slide 8 Well Polymer Coverslip	ibidi GmbH #80826
BD FACSCelesta™ Cell Analyzer	BD Biosciences #23-17410-00
GFP Monoclonal Antibody (5F12.4), eFluor 660, eBioscience™	Thermo Fisher Scientific #50-6498-82
RNeasy® Mini Kit	Qiagen #74106
M-MuLV Reverse Transcriptase	New England BioLabs, Inc. #M0253
TaqMan™ RNase P Detection Reagents Kit	Thermo Fisher Scientific #4316831
LightCycler® 480 Probes Master	Roche Life Science #04707494001
LightCycler® 480 II	Roche Life Science #05015278001

Supplementary table 2: list of primers used in this research. Bases denoted in red are not complementary to the template. I = inosine. FAM and TAMsp are the reporter dye and quencher of the probe.

Name	Use	Sequence
F1	NL4.3 EnvGFP amplification for LTR-TAT insert	CCACAATAGAAAGAGCAGAAGACAGT
R2	NL4.3 EnvGFP amplification for LTR-TAT insert	GCTACTTGTGATTGCTCCATGT
F3	NL4.3 EnvGFP amplification for CMV insert	CATGAATTCAGAAGACAGTGGCAATG
R4	NL4.3 EnvGFP amplification for CMV insert	GTCTCGAGATACTGCTCCC
F5	LTR-TAT backbone inverse PCR for InFusion	AGCGGCCTCGAGACCTAGAAAAACATG
R6	LTR-TAT backbone inverse PCR for InFusion	ATGGTTGTGGCCATATTATCATCGTGT
F7	NL4.3 EnvGFP amplification for LTR-TAT InFusion	TATGGCCACAACCATATGAGAGTGAAGGAG AAGTATCAGC
R8	NL4.3 EnvGFP amplification for LTR-TAT InFusion	GGTCTCGAGGCCGCTTTATAGCAAAATCCTT TCCAAGCC
F13	Site directed mutagenesis; insert kozak in CMV-EnvGFP	CGAATTCAGAAGACAGTGGCCACCATGAGA GTGAAGGAGAA
R14	Site directed mutagenesis; insert kozak in CMV-EnvGFP	CTTCTCCTTCACTCTCATGGTGGCCACTGTCT TCTGAATTCG
Env F qPCR	RT-qPCR for NL4.3 Env	TTC TTI GGA GCA GCI GGA AGC ACI ATG G
Env R qPCR	RT-qPCR for NL4.3 Env	TTR ATG CCC CAG ACI GTI AGT TIC AAC
Env P qPCR	RT-qPCR for NL4.3 Env	/56-FAM/TGA CGC TGA CGG TAC AGG CCA GAC A/36-TAMSp/

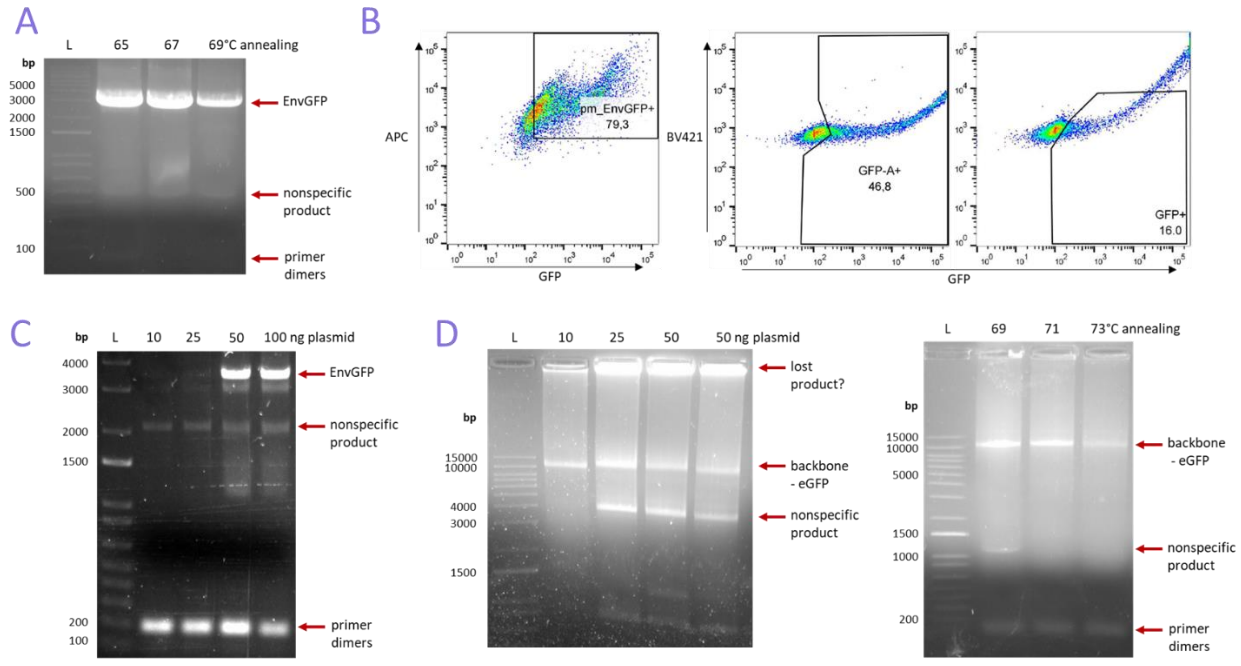

Supplementary fig. 1: cloning of lentiviral EnvGFP vectors. A: amplification of EnvGFP for insertion into the pHR' CMV expression vector. Optimal yield and product specificity was achieved with an annealing temperature of 67°C. B: transfection of a CMV-driven HBX2 Env V5.3 GFP OPT vector (left), the LTR-TAT GFP vector and the pHR CMV-GFP vector into HEK293T cells. Analysis by flow cytometry with α-GFP surface staining (left only). C: amplification of EnvGFP for insertion into the LTR-TAT-driven expression vector. Optimal yield and product specificity was achieved with 1 ng/µL (50 ng) template. D: inverse PCR of the LTR-TAT-driven expression vector with varying amounts of template DNA (left) and annealing temperatures (right). Optimal yield and product specificity were achieved with 0.2 ng/µL (10 ng) template and an annealing temperature of 71°C.

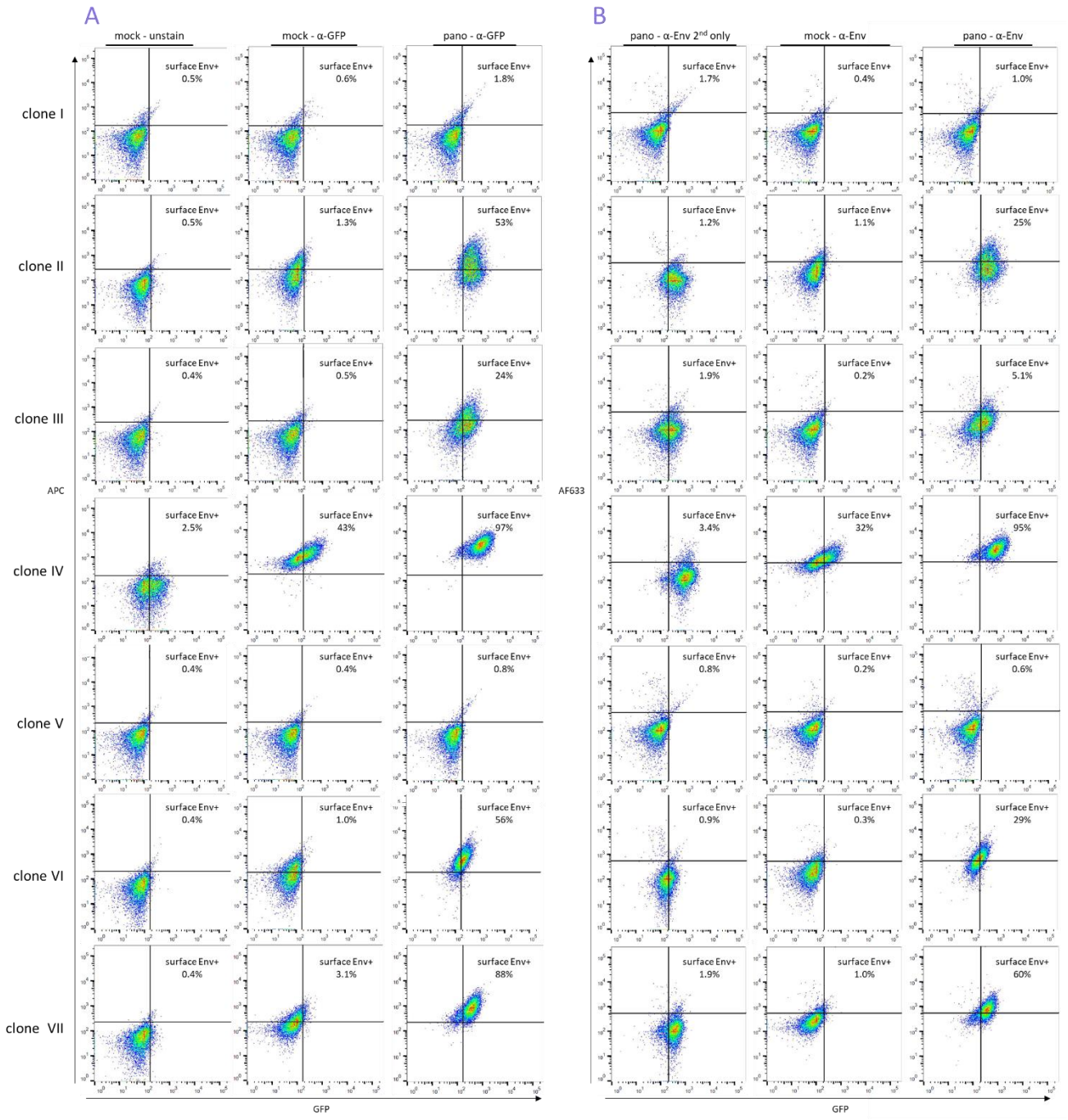

Supplementary fig. 2: reactivation of LTR-TAT EnvGFP Jurkat T-cell clones obtained by FACS. Cells were reactivated by treatment with Panobinostat, subjected to α-GFP (A) and α-Env (B) surface staining before flow cytometric analysis.